The climatology of Brewer-Dobson circulation and the contribution of gravity waves

Kaoru Sato[1], Soichiro Hirano[1]

[1]Department of Earth and Planetary Science, the University of Tokyo, Tokyo 113-0033, Japan

5 *Correspondence to*: Kaoru Sato (kaoru@eps.s.u-tokyo.ac.jp)

Abstract. The climatology of residual mean circulation, which is a main component of Brewer-Dobson circulation, and the potential contribution of gravity waves (GWs) are examined for the annual mean state and for each season based on the transformed-Eulerian mean zonal momentum equation using modern four reanalysis data, which allows us to examine the whole stratosphere. First, the potential contribution of Rossby waves (RWs) to residual mean circulation is estimated from

10 Eliassen-Palm flux divergence. The rest of residual-mean circulation, from which the potential RW contribution and zonal mean zonal wind tendency are subtracted, is regarded as the potential GW contribution. These potential wave contributions are exact contributions for the annual mean state and give good approximates for solstitial seasons. The GWs contribute to drive not only the summer hemispheric part of the winter deep branch and low-latitude part of shallow branches, as indicated by previous studies, but also cause a higher-latitude extension of the deep circulation in all seasons except for summer. This

15 GW contribution is essential to determine the location of the turn-around latitude. The autumn circulation is stronger and wider than that of spring in the equinoctial seasons, regardless of almost symmetric RW and GW contributions around the equator. This asymmetry is attributable to the existence of the spring-to-autumn pole circulation corresponding to the angular momentum transport associated with seasonal variation due to the radiative process. The potential GW contribution is larger in September-to-November than in March-to-May in both hemispheres. The upward mass flux is maximized in the boreal

20 winter in the lower stratosphere, while it exhibits semi-annual variation in the upper stratosphere. The GW contribution to the annual mean upward mass flux is in a range of 10–30 %, depending on the reanalysis data. The boreal winter maximum in the lower stratosphere is attributable to stronger RW activity in both hemispheres than in the austral winter.

1 Introduction

The meridional circulation in the middle atmosphere is an important component of the earth's climate, which globally

25 transports minor constituents and causes adiabatic heating/cooling via the downwelling/ upwelling. Part of the middle atmosphere has a thermal structure that is considerably different from the state of radiative equilibrium. The middle atmosphere circulation is mainly wave-driven. While gravity waves (GWs) are a primary driver of the mesospheric summer pole-to-winter pole circulation, Rossby waves (RWs), including planetary waves and synoptic-scale waves, are most important for driving the stratospheric circulation called Brewer-Dobson circulation (BDC). BDC consists of relatively-slow residual-mean

circulation driven by the wave forcing and rapid isentropic mixing with the turbulence associated with wave breaking and instability (Butchart, 2014). Residual mean circulation is divided into one deep and two shallow branches (e.g., Birner and Bönisch, 2011). The deep branch located in the winter middle and upper stratosphere is essentially driven by planetary waves and two shallow branches in the lower stratosphere of both hemispheres by synoptic-scale waves (e.g., Plumb, 2002). However,

5 these descriptions are a rough sketch of BDC.

Recent advanced research tools, such as reanalysis data based on modern data-assimilation systems, have enabled the BDC structure to be examined in detail and have highlighted the role of GW forcing even in the stratosphere (e.g., Butchart, 2014; Okamoto et al., 2011; Seviour et al., 2012). Another useful tool for the analysis is the downward control principle derived by Haynes et al. (1991). This principle indicates that the Coriolis torque for the residual mean meridional flow is balanced

10 with the wave forcing in a steady state. The contribution of each wave to the residual mean flow can be evaluated using this principle (McLandress and Shepherd, 2009). Okamoto et al. (2011) applied this method to the ERA-Interim data (Dee et al., 2011) and to the outputs of a chemistry climate model (CCM) and showed that the GW forcing contributes to the formation of the summer hemispheric part of the deep branch of the winter circulation where RWs hardly propagate in the mean easterly wind of the summer stratosphere (Charney and Drazin, 1961), and to the formation of the shallow branches where orographic

15 GWs break in the weak wind layer in the lower stratosphere (Lilly and Kennedy, 1973; Sato, 1990; Tanaka, 1986).

The upward mass flux is a quantity describing the strength of BDC. Previous studies showed that the upward mass flux exhibits an annual cycle with a maximum in the boreal winter (e.g., Randel et al., 2008). Seviour et al. (2012) used the ERA-Interim data and estimated the contribution of parameterized orographic GW forcing to the upward mass flux at 70 hPa associated with the residual mean circulation at ~4 % which is much smaller than the difference (~30 %) between the total

20 mass flux and the contribution of resolved wave forcing. They suggested the significant contribution of unresolved waves, such as non-orographic GWs. Chun et al. (2011) used WACCM climatological simulation data and showed that GWs contribute to the upward mass flux by 17 % at 70 hPa with comparable contributions by convective and orographic GWs. They estimated the contribution of GWs, by taking the zonal mean zonal wind tendency in the zonal mean zonal momentum equation into consideration following Randel et al. (2008). These previous studies discussed the structure and strength of BDC only in

25 the lower stratosphere, and its structure in the middle and upper stratosphere has not yet been examined in detail.

The contribution of respective waves was examined for data from future projections by CCMs in a framework of the model intercomparison (Butchart et al., 2010). The results indicate that most CCMs project the acceleration of residual mean circulation in the stratosphere. Although the projected increase in the strength of the circulation did not significantly differ among the models, the ratio of the resolved and unresolved wave contributions largely depended on the model. As a plausible

30 mechanism to explain this puzzling result, Cohen et al. (2013) showed the potential compensation of the parameterized GW forcing due to the barotropic and/or baroclinic instability in the model: any excess of the parameterized GW forcing can be adjusted by the instability processes, and hence the contribution of GW forcing in a projected climate is hardly estimated in the model. However, it is worth noting here that the analysis on BDC in the past and present climate using reanalysis data may

not be impacted considerably by this problem even if GW parameterizations are not perfect, as the analyzed dynamical fields should be realistic through the assimilation of a large amount of observation data.

The application of the method using the downward control principle to estimate respective wave contributions is not appropriate to the analysis of tropical regions because this method assumes a balance between the Coriolis torque and wave forcing (i.e., the Coriolis parameter is not zero). In addition, radiative heating needs to be considered for tropical regions in solstitial seasons. The observed temperature in tropical regions is almost uniform latitudinally even in the solstitial seasons when and where the latitudinal gradient of radiative heating by ozone is not negligible. This suggests the presence of thermally-driven circulation called the middle atmosphere Hadley circulation, which was first indicated and examined by Dunkerton (1989) and revisited by Semeniuk and Shepherd (2001). The middle atmosphere Hadley circulation is confined at latitudes lower than 30° and composed of a summer-to-winter hemisphere cell with an upward (downward) blanch in the summer (winter) hemisphere. This cell merges with the deep winter circulation formed by the westward forcing due to the RWs in the middle- and high-latitude regions. As for the wave contribution in the low-latitude region, Kerr-Munslow and Norton (2006) and Norton (2006) indicated that the equatorial RWs generated by strong tropical convection cause significant wave forcing in the off-equatorial region and suggests its large effects on the upwelling. However, the forcing by equatorial RWs cannot form the equatorward flow in the summer low-latitude region like the middle atmosphere Hadley circulation driven by differential radiative heating because the forcing by dissipating RWs is westward. In contrast, the forcing associated with GW dissipation and/or breaking can be positive and cause the equatorward flow in the summer subtropical region, as suggested by Okamoto et al. (2011).

Another limitation of the analysis using the downward control principle is the assumption of a steady state. For this reason, the driving force of the residual mean circulation in the equinoctial seasons has not been examined in detail. For example, Seviour et al. (2012) showed the structure of the residual mean circulation in the equinoctial seasons but did not discuss its details. According to their Fig. 3, even in the equinoctial seasons, the circulation is not symmetric around the equator in the stratosphere. It should be meaningful to elucidate the details on the physics of the circulation with such a structure. Particularly for the equinoctial seasons, the time change (tendency) of zonal mean zonal wind, which is ignored in the downward control principle analysis, needs to be considered in addition to the wave forcing in the zonal mean zonal momentum equation. A potential method to overcome this issue is that proposed by Randel et al. (2008), as described above. The present study will examine the tendency of zonal mean zonal wind with an expression of the stream function. This expression gives an angular momentum transport, which should be prevailing during a seasonal transition from the summer easterly to the winter westerly and vice versa in the middle atmosphere.

This paper focuses on two new aspects of the residual mean circulation in the stratosphere, which is a main part of BDC. One aspect is the climatological features of the potential GW contribution to the residual mean circulation in the whole stratosphere for the annual mean state and for each season. For this purpose, four modern reanalysis datasets over 30 years are analyzed. The climatological features are discussed in terms of the stream function structure and the upward mass flux. The interplay of RWs and GWs for the residual mean circulation is also highlighted. Particularly, the characteristics of potential

GW contributions in equinoctial seasons are first shown by this study. We define them as "potential" because the wave forcing in the zonal momentum equation is not merely balanced with the Coriolis force for the residual mean meridional flow but also causes the acceleration of the zonal mean zonal wind.

The other new aspect upon which we focus is the climatological structure of the residual mean circulation in the middle and upper stratosphere, which have not yet been examined well by previous studies, even for the solstitial seasons when the steady assumption is generally valid. The analysis for this region has recently been feasible with the aid of the modern reanalysis data using high-top models in the assimilation system, like NASA Modern Era Reanalysis for Research and Applications (MERRA) (Rienecker et al., 2011) and MERRA Version 2 (MERRA-2) (Gelaro et al., 2017).

Note that this study is positioned as a part of the WCRP/SPARC S-RIP project. Thus, a comparison among the four reanalysis datasets is also made. As the GWs are subgrid-scale phenomena in most models used for the reanalysis, the GW contributions can be estimated only indirectly. Thus, the difference among the reanalysis data must be meaningful.

An analysis is performed using four reanalysis datasets: MERRA, MERRA-2, ERA-Interim, and JRA-55 (Kobayashi et al., 2015). Descriptions are mainly made using MERRA-2 data because the model's top level 0.01 hPa of MERRA and MERRA-2 is higher than that of ERA-Interim and JRA55 (0.1 hPa), and because MERRA-2 is newer than MERRA. The method of the analysis and a brief description of analyzed data are given in section 2. The characteristics of the annual mean and seasonal mean stream functions are described, and the contributions of RWs and GWs are discussed in section 3. The characteristics of seasonal variations in the upward mass flux are shown and the contributions of RWs and GWs are discussed in section 4. Section 5 discusses the seasonal variations in the potential GW contribution to the residual mean circulation by comparing the results by previous observational studies of GWs. Section 6 includes the summary and concluding remarks.

2 Method of analysis

Considering that RWs are realistically expressed in the reanalysis data and that the grid spacing of the reanalysis data is still coarse to express GWs, the resolved (subgrid-scale) waves are designated as RWs (GWs). Thus, the divergence of the Eliassen-Palm (EP) flux ($\boldsymbol{F}$), $\nabla \cdot \boldsymbol{F}$, directly calculated using the reanalysis data, is regarded as the RW forcing. Similar to Randel et al. (2002), we use the zonal mean zonal momentum equation in the transformed-Eulerian mean (TEM) equation system for the spherical coordinates (Andrews et al., 1987),

$$-\hat{f}\overline{v}^* + \overline{w}^* \frac{\partial \overline{u}}{\partial z} = \frac{1}{\rho_0 a \cos \phi} \nabla \cdot \boldsymbol{F} + \overline{X} - \frac{\partial \overline{u}}{\partial t}, \qquad (1)$$

to evaluate the residual mean flow ($\overline{v}^*, \overline{w}^*$), where $\overline{X}$ is mainly the forcing caused by GWs (hereafter referred to as the GW forcing);

$$\hat{f} \equiv f - \frac{1}{a \cos \phi} \frac{\partial (\overline{u} \cos \phi)}{\partial \phi} = 2\Omega \sin \phi - \frac{1}{a \cos \phi} \frac{\partial (\overline{u} \cos \phi)}{\partial \phi}; \qquad (2)$$

z is the log pressure height, and ϕ is the latitude. The sum of the first and second terms in the right side of Eq. (1) is referred to as the wave forcing. The meridional ($\overline{v}^*$) and vertical ($\overline{w}^*$) components of the residual mean flow are respectively defined as

$$\overline{v}^* \equiv \overline{v} - \frac{1}{\rho_0}\left(\rho_0 \frac{\overline{v'\theta'}}{\theta_{0z}}\right)_z \quad \text{and} \quad \overline{w}^* \equiv \overline{w} + \frac{1}{a\cos\phi}\left(\cos\phi \frac{\overline{v'\theta'}}{\theta_{0z}}\right)_\phi. \tag{3}$$

See Andrews et al. (1987) for the formulae for $\boldsymbol{F}$ [their equation (3.5.3)]. Other notations throughout in this work except for those defined explicitly are standard, following Andrews et al. (1987).

The residual-mean flow gives an approximate but direct estimate of the Lagrangian mean flow (i.e., the sum of Eulerian mean flow and Stokes drift) according to the small-amplitude theory. From the continuity equation, a stream function Ψ of the residual mean flow is defined as

$$\overline{v}^* \equiv -\frac{1}{\rho_0\cos\phi}\Psi_z, \quad \text{and} \quad \overline{w}^* \equiv \frac{1}{\rho_0 a\cos\phi}\Psi_\phi. \tag{4}$$

Thus, there are two methods to estimate $\Psi(\phi,z)$ directly from Eq. (4): One is an integration of $\overline{v}^*$ in the vertical with a top boundary condition of $\Psi = 0$. The other is a latitudinal integration of $\overline{w}^*$ with a boundary condition of $\Psi = 0$ at the North Pole or the South Pole. In this study, $\Psi(\phi,z)$ in the Northern Hemisphere (NH) [Southern Hemisphere (SH)] by the latitudinal integration of $\overline{w}^*$ starting $\Psi = 0$ at the North [South] Pole. The comparison of the two methods is discussed in Appendix A. Hereafter, Ψ is called the total stream function to distinguish from the stream functions of wave contributions.

The contribution of each term in Eq. (1) to the total stream function is evaluated as follows. First, substitution of Eq. (4) into Eq. (1) yields

$$\frac{\partial(\Psi,\overline{m})}{\partial(\phi,z)} = \left(\frac{1}{\rho_0 a\cos\phi}\nabla\cdot\boldsymbol{F} + \overline{X} - \frac{\partial\overline{u}}{\partial t}\right)\rho_0 a^2\cos^2\phi, \tag{5}$$

where $\overline{m} = a\cos\phi\,(\overline{u} + a\Omega\cos\phi)$ is the zonal mean angular momentum per unit mass (Haynes et al., 1991; Randel et al., 2002). Using Eq. (5), $\Psi(y,z)$ is expressed as a sum of three components:

$$\Psi(\phi,z) = \Psi_{\text{RW}}(\phi,z) + \Psi_{\text{GW}}(\phi,z) + \Psi_{\text{dU/dt}}(\phi,z) \tag{6}$$

where

$$\Psi_{\text{RW}}(\phi,z) \equiv -\int_z^\infty \left[\frac{\nabla\cdot\boldsymbol{F}}{a\hat{f}}\right]_{\overline{m}} d\zeta, \tag{7}$$

$$\Psi_{\text{GW}}(\phi,z) \equiv -\cos\phi\int_z^\infty \left[\frac{\rho_0}{\hat{f}}\overline{X}\right]_{\overline{m}} d\zeta, \tag{8}$$

$$\Psi_{\text{dU/dt}}(\phi,z) \equiv \cos\phi\int_z^\infty \left[\frac{\rho_0}{\hat{f}}\frac{\partial\overline{u}}{\partial t}\right]_{\overline{m}} d\zeta, \tag{9}$$

and $\int_z[\quad]_{\overline{m}}d\zeta$ means a vertical integration along a constant $\overline{m}$. With this vertical integration instead of that along a constant ϕ, the vertical advection of zonal wind $\overline{w}^*\frac{\partial\overline{u}}{\partial z}$ in Eq. (1) can be included for the estimation. In this study, $\Psi_{\text{RW}}(\phi,z)$ and

$\Psi_{GW}(\phi, z)$ are respectively called potential RW and GW contributions to the residual mean flow. We used the "potential" contribution because the wave forcings drive the residual mean flow, but a part of them causes acceleration/deceleration of $\overline{u}$ [i.e., $\partial \overline{u}/\partial t$ in Eq. (1)]. The distribution of the wave forcing to the Coriolis term $-\hat{f}\overline{v}^*$ and the tendency term $\partial \overline{u}/\partial t$ depends on the aspect ratio of the forcing in the meridional cross section soon after the forcing is given (Garcia, 1987; Hayashi and Sato, 2018). The part of the stream function by the zonal mean zonal wind tendency is expressed as $\Psi_{dU/dt}(\phi, z)$. The $\Psi_{GW}(\phi, z)$ cannot be directly calculated because of the unknown $\overline{X}$, but it can indirectly be estimated using

$$\Psi_{GW}(\phi, z) = \Psi(\phi, z) - \Psi_{RW}(\phi, z) - \Psi_{dU/dt}(\phi, z). \qquad (10)$$

In this study, the integrations in Eqs. (7) and (9) were performed faithfully along the angular momentum ($\overline{m}$) contour in the vertical because the contribution of GW forcing is expected relatively small and hence the uncertainty should be reduced as much as possible, although a few previous studies performed an approximated integration at a constant ϕ in the vertical (McLandress and Shepherd, 2009; Okamoto et al., 2011). Note that as $\hat{f}$ is quite small near the equator, the stream functions of Eq. (7), Eq. (9), and Eq. (10) are obtained for $|\phi| > 20°$.

Under the steady state assumption, which is valid for the annual mean and approximately valid for the solstitial seasons, Eqs. (7) and (8) are reduced to the downward control principle by Haynes et al. (1991) (Randel et al., 2002). In this case, $\Psi_{RW}(\phi, z)$ and $\Psi_{GW}(\phi, z)$ are exact contributions by RWs and GWs (McLandress and Shepherd, 2009).

The zonal mean zonal wind tendency $\partial \overline{u}/\partial t$ is large in the equinoctial seasons because of the seasonal change in the radiative heating. As the seasonal time scale is much longer than a typical radiative relaxation time in the stratosphere, the wave forcing hardly causes $\partial \overline{u}/\partial t$ and is almost balanced with a part of $-\hat{f}\overline{v}^*$ except for the equatorial region where the Coriolis parameter f is quite small. Thus, the zonal mean zonal wind tendency term $\partial \overline{u}/\partial t$ is evaluated as the radiation effect, which should be balanced with the Coriolis force for the residual mean flow similar to the wave forcing. In this study, $\Psi_{RW}(\phi, z)$ and $\Psi_{GW}(\phi, z)$ will mainly be discussed as respective wave contributions to the residual mean circulation, and the potential contributions of RWs and GWs to $\partial \overline{u}/\partial t$ will also be noted.

Next, the method of upward mass flux is described. In the steady state, the amount of upward mass flux $F^\uparrow(z)$ should be balanced with the sum of downward mass fluxes in the NH ($F^\downarrow_{NH}$) and SH ($F^\downarrow_{SH}$):

$$F^\uparrow(z) = -[F^\downarrow_{NH}(z) + F^\downarrow_{SH}(z)], \qquad (11)$$

$$F^\downarrow_{NH}(z) = 2\pi a^2 \rho_0 \int_{\phi^{NH}_{TL}}^{\frac{\pi}{2}} \overline{w}^*(z) \cos\phi \, d\phi = 2\pi a \Psi(\phi^{NH}_{TL}, z), \qquad (12)$$

$$F^\downarrow_{SH}(z) = 2\pi a^2 \rho_0 \int_{-\frac{\pi}{2}}^{\phi^{SH}_{TL}} \overline{w}^*(z) \cos\phi \, d\phi = -2\pi a \Psi(\phi^{SH}_{TL}, z), \qquad (13)$$

where ϕ^{NH}_{TL} and ϕ^{SH}_{TL} are the turn-around latitudes where $\overline{w}^* = 0$ for the NH and SH circulations at each altitude, respectively. Eqs. (11)–(13) indicate that the total upward mass flux and the contributions by the NH and SH are estimated only using stream function values at the turn-around latitudes. Using $\Psi_{RW}(\phi, z)$ and $\Psi_{GW}(\phi, z)$ in place of $\Psi(\phi, z)$, the RW and GW

contributions to the upward mass flux are estimated, respectively. For equinoctial seasons when the steady state assumption does not hold, this method only estimates the potential contributions by the RWs and GWs.

Four reanalysis datasets of MERRA-2, MERRA, JRA-55, and ERA-Interim over 30 years from 1986–2015 are used to examine the climatology of the residual mean circulation in the whole stratosphere as the main part of BDC. Although the horizontal resolutions of the model used for the data assimilation are different (Fujiwara et al., 2017), the grid intervals are almost the same for the four reanalyses (1.25°×1.25° for MERRA, MERRA-2, and JRA-55, and 1.5°×1.2° for ERA-Interim). Thus, the horizontal wavenumber range of "resolved waves" examined in the present study is almost the same for all reanalysis datasets. The top of the model is 0.01 hPa for MERRA and MERRA-2 and 0.1 hPa for ERA-Interim and JRA-55. Features for the annual mean state and for the four seasons of December to February (DJF), March to May (MAM), June to August (JJA), and September to November (SON) are analyzed.

3 Results

Before the details of the circulation for the annual mean state and for each season are discussed, the meridional cross sections of the zonal mean zonal wind climatology are shown in Fig. 1, as both RW and GW propagations strongly depend on the mean wind. Since the difference in the stratospheric mean wind is not large among the reanalysis data, and the detailed comparison of the mean wind itself is beyond the scope of this study, only the field from MERRA-2, which covers the region up to the highest level, is shown. As is well known, the winter westerly jet is stronger in the SH (JJA) than in the NH (DJF). In spring, the westerly jet is strong and has a peak in the lower stratosphere in the SH (SON), while the westerly jet almost disappears in the NH (MAM). These differences in the westerly jet between the two hemispheres are considered as the result of the different activity of RWs generated in the troposphere. Another interesting difference is the strength of the summer easterly jet, which is stronger in the SH (DJF) than in the NH (JJA). This feature is not very well known, but it could be valuable to examine the cause in future studies.

3.1 Annual mean structure of the stream functions

Figure 2 shows the latitude-height sections of annual mean values of $\Psi(\phi, z)$, $\Psi_{RW}(\phi, z)$, and $\Psi_{GW}(\phi, z)$ for all the reanalysis data. There are many notable interesting and important characteristics that are commonly observed in all datasets. In this and subsequent sections, first, the characteristics observed in the new reanalysis MERRA-2 covering the wide height region are discussed, and next, differences among the four datasets are described.

As is well known, two-celled circulation is clearly observed for the annual-mean total stream function $\Psi(\phi, z)$, which is directly estimated using Eqs. (3) and (4), in Fig. 2a. The $\Psi(\phi, z)$ in the NH has slightly larger magnitudes than in the SH in most stratosphere below 2 hPa. This feature is consistent with stronger planetary-scale RW activity in the NH (Fig. 2b). In fact, the two-celled circulation in $\Psi(\phi, z)$ is mainly determined by the RW contribution, $\Psi_{RW}(\phi, z)$. However, the GW contribution, $\Psi_{GW}(\phi, z)$, is also important in some notable regions (Fig. 2c) as described in the following.

The GW contribution is almost symmetric around the equator with a slight hemispheric difference. The GWs contribute largely to the poleward circulation [i.e., clockwise (counter-clockwise) circulation in the NH (SH)] in the middle- and high-latitude regions of the whole stratosphere. This circulation should be caused by the westward forcing due to GWs likely originating from the topography and jet-front system in the troposphere (e.g., Hertzog et al., 2008; Sato et al., 2009; Shibuya et al., 2015). The magnitude of $\Psi_{GW}(\phi, z)$ in the poleward circulation is slightly larger in the SH than in the NH.

In addition, a characteristic equatorward circulation [i.e., counter-clockwise (clockwise) circulation in the NH (SH)] is observed in the low-latitude region in $\Psi_{GW}(\phi, z)$ whose largest latitudinal extension to 30° at 10 hPa. This equatorward circulation is caused by the eastward forcing due to GWs, which likely originate from vigorous convection in the subtropical region (e.g., Pfister et al., 1993; Sato et al., 2009). It is also worth noting that the turn-around latitude of the poleward circulation for $\Psi_{GW}(\phi, z)$ is observed at approximately 40–55 degrees depending on the altitude, which is higher than that in $\Psi_{RW}(\phi, z)$. This means that the GW forcing can modify the turn-around latitude of the BDC, as discussed in detail later.

The characteristics of $\Psi(\phi, z)$, $\Psi_{RW}(\phi, z)$, and $\Psi_{GW}(\phi, z)$ described above are similarly observed in other reanalysis data. However, there are a few differences. One is in the equatorward circulation in the low-latitude region for $\Psi_{GW}(\phi, z)$: The circulation extends down to 100 hPa for MERRA and MERRA-2, the lower end of the circulation is located at 20–30 hPa for ERA-Interim, and the circulation itself is not clear for JRA-55. Instead, the $\Psi_{GW}(\phi, z)$ for ERA-Interim and JRA-55 exhibits strong poleward circulation below 30 hPa in the low- and middle-latitude regions. Similar strong poleward circulation is observed only in the middle-latitude region for MERRA and MERRA-2. This strong circulation probably reflects the orographic GW forcing enhanced in the weak wind layer above the subtropical jet (Lilly and Kennedy, 1973; Sato, 1990; Tanaka, 1986).

The other difference is observed in $\Psi_{RW}(\phi, z)$, which is deeper for MERRA/MERRA-2 than for ERA-Interim/JRA-55. One potential reason for this is the difference in the top of the model used for the data assimilation (0.01 hPa for MERRA/MERRA-2 and 0.1 hPa for ERA-Interim/JRA-55) and hence the data top (0.1 hPa for MERRA/MERRA-2 and 1 hPa for ERA-Interim/JRA-55). Thus, the top of the vertical integration in Eq. (7) depends on the reanalysis data, and the underestimation of $\Psi_{RW}(\phi, z)$ by ignoring the RW forcing above the data top can be greater for ERA-Interim/JRA-55 than that for MERRA/MERRA-2. This inference is consistent with the deeper $\Psi_{RW}(\phi, z)$ for the reanalysis data with a higher top, suggesting that the RW forcing in the upper stratosphere and mesosphere is not negligible fin the upper stratospheric circulation.

There are other potential elements causing these differences in the stream function among the reanalysis data. One is the GW parameterizations used the assimilation system: The models for ERA-Interim and JRA-55 use both orographic and non-orographic GW parameterizations, while only non-orographic GW parameterizations are used for MERRA and MERRA-2. Any potential difference caused by the parameterized GW forcing should be corrected by the increment given by the data assimilation system. However, the observation data used for the data assimilation are not sufficient, and the correction may not be perfect. The other element is the assimilation method, which is the 4d-Var for ERA-Interim and JRA-55 and the 3d-Var for MERRA and MERRA-2. However, a detailed investigation on the reasons for the differences in the stream function among the four analysis datasets is beyond the scope of this paper and is left for future studies.

Next, the annual mean $\Psi(\phi, z)$, $\Psi_{RW}(\phi, z)$, and $\Psi_{GW}(\phi, z)$ are more closely examined as a function of the latitude, focusing on three levels: 70 hPa, 10 hPa, and 3hPa in Figs. 3, 4 and 5, respectively. The positive and negative maxima in $\Psi(\phi)$ (black curves) corresponding to the turn-around latitudes are almost the same for all reanalysis data for 70 hPa that are at $\phi_{TL}^{NH} = \sim 35^{\circ}N$ and at $\phi_{TL}^{SH} = \sim 30^{\circ}S$. The magnitudes of $\Psi_{RW}(\phi)$ (blue curves) are almost the same for all reanalysis data. It is

5   important and interesting that $\Psi_{RW}(\phi)$ is flat and does not have clear peaks near the turn-around latitudes of $\Psi(\phi)$, although RW is considered as a primary driver of BDC. Instead, the turn-around latitudes of $\Psi(\phi)$ are mainly determined by the shape of $\Psi_{GW}(\phi)$ (red curves).

The importance of GWs is also the case for 10 hPa (Fig. 4). The turn-around latitudes of $\Psi(\phi)$ at 10 hPa are located at $\phi_{TL}^{NH} = 30^{\circ}N$ and at $\phi_{TL}^{SH} = 35^{\circ}S$. The $\Psi_{RW}(\phi)$ has the maxima but at lower latitudes ($25^{\circ}N$ and $25^{\circ}S$) than ϕ_{TL}^{NH} and ϕ_{TL}^{SH} for

10   all reanalysis data, although the magnitude depends on the data. The sharp increase with the latitude in $\Psi_{GW}(\phi)$ observed up to 50 degrees largely contributes to determining the location of the turn-around latitudes. The determination of the turn-around latitudes is an important role of GWs in the annual mean residual circulation.

The difference in the magnitude and shape of $\Psi(\phi, z)$, $\Psi_{RW}(\phi, z)$, and $\Psi_{GW}(\phi, z)$ among the four reanalysis datasets is much larger at 3 hPa (Fig. 5) than at lower levels, although a similar GW contribution to the location of the turn-around

15   latitudes is observed at this level. The difference among the datasets may be again due to the limitation of the data assimilation owing to the model performance and/or insufficient observation data. Thus, a further detailed description is not provided for 3 hPa.

3.2 Stream functions in solstitial seasons

20   Figure 6 (Fig. 7) shows the climatology of $\Psi(\phi, z)$, $\Psi_{RW}(\phi, z)$, $\Psi_{GW}(\phi, z)$, and $\Psi_{dU/dt}(\phi, z)$ for DJF (JJA) obtained by each reanalysis dataset. As is widely known, it is seen that the winter circulation in $\Psi(\phi, z)$ is deep and stronger and extends to the summer hemisphere, while the summer circulation is strong only in the lower and middle stratosphere.

It is seen from the comparison among $\Psi(\phi, z)$, $\Psi_{RW}(\phi, z)$ and $\Psi_{GW}(\phi, z)$ for MERRA-2 (Figs. 6a–6d) that the major part of $\Psi(\phi, z)$ is attributed to the RW forcing. However, the GW contribution is also large: The GWs contribute to the

25   formation of the summer hemispheric part of the winter circulation, as indicated by Okamoto et al. (2011). In particular, the upper stratospheric part in the whole summer hemisphere is mainly determined by the GWs. It is interesting that the GW contribution in the summer upper stratosphere in the NH and that in the SH are comparable. Thus, the GW forcing in the region analyzed in the stratosphere may not be responsible for the significant difference in the mean easterly wind in summer between the NH (JJA) and SH (DJF) (Figs. 1c and 1a), as indicated earlier. Another notable feature in the circulation toward the winter

30   pole is that the extension of the winter circulation to the high latitudes is explained by the GW forcing. This feature is clearer for the SH (JJA) where the $\Psi_{RW}(\phi, z)$ values are quite small or almost zero in the middle and upper stratosphere.

The poleward circulation in the summer hemisphere is deeper and stronger in the SH (DJF) than in the NH (JJA). This hemispheric difference is mainly due to larger RW contribution in the SH. This is consistent with the feature observed in the mean wind in which a relatively strong westerly mean wind remains in the lower stratosphere in the SH (DJF) (Fig. 1a). This westerly mean wind allows RWs from the troposphere to reach the lower stratosphere.

5   Compared with $\Psi(\phi, z)$, $\Psi_{\mathrm{dU/dt}}(\phi, z)$ for the solstitial seasons is quite small except summer low latitudes. This fact ensures the validity of the steady state assumption for solstitial seasons, which are frequently made for the diagnostics using the downward control principle (e.g., McLandress and Shepherd, 2009). It is interesting that the magnitude of $\Psi_{\mathrm{dU/dt}}(\phi, z)$ in the summer low-latitude region is comparable to that of $\Psi_{\mathrm{GW}}(\phi, z)$ but confined in the lower stratosphere. The direction and latitudinal location of this circulation are consistent with the middle atmosphere Hadley circulation, although dominant altitude

10 region may be slightly lower than the theoretical expectation (i.e., upper stratosphere) (Semeniuk and Shepherd, 2001). It is also worth noting that there is a weak equatorward circulation in $\Psi_{\mathrm{dU/dt}}(\phi, z)$ in the winter hemisphere, which is located in the middle-latitude region in the NH (DJF) and at relatively low latitudes in the SH (JJA). Equatorward circulation in $\Psi_{\mathrm{dU/dt}}(\phi, z)$ means westerly wind weakening. Thus, these equatorward circulations in $\Psi_{\mathrm{dU/dt}}(\phi, z)$ can be at least partly due to the strong westward RW forcing in the winter stratosphere and the summer lower stratosphere. The difference in the

15 dominant-latitude region of $\Psi_{\mathrm{dU/dt}}(\phi, z)$ for the winter season between the two hemispheres is consistent with this inference.

       The overall characteristics in solstitial seasons described above for MERRA-2 are similarly observed in other reanalysis datasets. However, there are some differences among the datasets, although they are minor. The poleward circulation in $\Psi(\phi, z)$ in summer is deeper in MERRA and MERRA-2 than in ERA-Interim and JRA-55. Counter circulation in the winter low-latitude region is observed in $\Psi_{\mathrm{GW}}(\phi, z)$ in MERRA and MERRA-2, while it is not for the other datasets. A similar

20 discussion for the annual mean climatology in section 3.1 would be made for these differences for the solstitial seasons.

3.3 Stream functions in equinoctial seasons

The zonal mean zonal wind tendency is large due to a seasonal change in the radiative heating in the equinoctial seasons. Thus, roughly speaking, $\Psi_{\mathrm{dU/dt}}(\phi, z)$ is primarily attributable to the radiation in the equinoctial seasons and the acceleration/deceleration by the wave forcing is secondary. Figure 8 (Fig. 9) shows the climatology of $\Psi(\phi, z)$, $\Psi_{\mathrm{RW}}(\phi, z)$,

25 $\Psi_{\mathrm{GW}}(\phi, z)$, and $\Psi_{\mathrm{dU/dt}}(\phi, z)$ for MAM (SON).

       The most interesting feature is that $\Psi(\phi, z)$ is not symmetric around the equator (Figs. 8a and 9a) regardless of the equinoctial seasons. The circulation structure rather resembles that in the subsequent solstitial season. The autumn circulation is stronger and latitudinally wider than the spring circulation. In contrast, $\Psi_{\mathrm{RW}}(\phi, z)$ (Figs. 8b, and 9c) and $\Psi_{\mathrm{GW}}(\phi, z)$ (Figs. 8c and 9c) are almost symmetric around the equator similar to the annual mean circulations (Figs. 2b and 2c), although the

30 strength is slightly different. The anti-symmetry around the equator observed in $\Psi(\phi, z)$ is attributable to the structure of $\Psi_{\mathrm{dU/dt}}(\phi, z)$. The circulation in $\Psi_{\mathrm{dU/dt}}(\phi, z)$ is globally southward (northward) in MAM (SON), in other words, from the

spring pole to the autumn pole. This is consistent with the angular momentum conservation for the easterly (westerly) jet formation in the spring (autumn) hemisphere.

Except for $\Psi_{GW}(\phi, z)$ in the low-latitude region, most of the $\Psi_{RW}(\phi, z)$, $\Psi_{GW}(\phi, z)$, and $\Psi_{dU/dt}(\phi, z)$ values have the same sign in the autumn hemisphere, while $\Psi_{dU/dt}(\phi, z)$ values has the opposite sign to those of $\Psi_{RW}(\phi, z)$ and $\Psi_{GW}(\phi, z)$

5   in the spring hemisphere. The difference in the magnitudes of $\Psi_{RW}(\phi, z)$ and $\Psi_{GW}(\phi, z)$ between the spring and autumn hemispheres is not large compared with that between the two hemispheres in the solstitial seasons, as already mentioned. Therefore, it is concluded that the stronger circulation expanding over a wider latitudinal region in the autumn hemisphere than in the spring one is mainly due to the seasonal change in the radiative heating.

Next, detailed contributions by RWs [$\Psi_{RW}(\phi, z)$], and GWs [$\Psi_{GW}(\phi, z)$] to the total circulation [$\Psi(\phi, z)$] are

10   discussed. In the lower stratosphere, the RW contribution [$\Psi_{RW}(\phi, z)$] is large and its magnitude is comparable to the radiation [$\Psi_{dU/dt}(\phi, z)$], whereas the GW contribution $\Psi_{GW}(\phi, z)$ is not negligible in the low-latitude region of the lowermost stratosphere. In the upper stratosphere, the GW contribution [$\Psi_{GW}(\phi, z)$] is rather dominant, particularly at the middle- and high-latitude regions where $\Psi_{RW}(\phi, z)$ is weak. Thus, the GW forcing is important to determine the turn-around latitudes and depth of the residual mean circulation in the equinoctial seasons similar to those for the annual mean circulation.

15   Another important feature in $\Psi(\phi, z)$ is that the spring circulation is stronger in the SH (SON) than in the NH (MAM), although the autumn circulation does not differ as much. This is mainly attributed to the stronger $\Psi_{RW}(\phi, z)$ in the SH (SON). It is interesting to note that $\Psi_{GW}(\phi, z)$ in spring is also stronger in the SH (SON) than in the NH (MAM), while it is comparable in autumn. These stronger RW and GW forcings in spring are reflected in the more distorted structure of $\Psi_{dU/dt}(\phi, z)$ in spring hemisphere than in the autumn one. It is also worth noting that the larger distortion in $\Psi_{dU/dt}(\phi, z)$ in spring in the SH (Fig.

20   9d) is consistent with the stronger RW activity than that in NH.

These characteristics of the equinoctial seasons in terms of the structure and contribution by wave forcing and radiative heating are similarly observed in the other reanalysis datasets, although there are some slight differences indicated for the annual mean circulation in section 3.1.

4. Seasonal variation of the upward mass flux

25   The total upward mass flux was estimated using Eqs. (11)–(13) for each month. In addition, contributions by RWs, GWs, and the zonal wind tendency are respectively calculated by replacing $\Psi(\phi, z)$ with $\Psi_{RW}(\phi, z)$, $\Psi_{GW}(\phi, z)$, and $\Psi_{dU/dt}(\phi, z)$ at the same turn-around latitudes determined by $\Psi(\phi, z)$. Figure 10 shows the results for 70 hPa for all reanalysis data. Black, red, and blue solid curves on the upper panel for each reanalysis dataset show the total upward mass flux and the contributions by the NH and SH, respectively. The RW contribution is shown by dashed curves, and the sum of RW and zonal wind tendency

30   contributions are shown by dotted curves. The bottom panel for each reanalysis dataset shows the percentage of the GW contribution. The asterisks on the right are the annual mean values. The left, middle, and right asterisks on the upper panel

show the mean values for the total upward mass flux, the RW contribution, and the RW plus zonal wind tendency contribution. Note again that the contributions by RWs and GWs shown in Fig. 10 give rough estimates because a part of RW and GW forcings is used to accelerate the zonal wind instead of driving the meridional circulation, as discussed in section 2.

The total upward mass flux is maximized in December and January (i.e., boreal winter) and minimized in June and July (i.e., austral winter). The boreal winter maximum is reflected by two features: First, the mass flux associated with the winter circulation is larger in the NH than in the SH, as is consistent with higher activity of planetary-scale RWs in the NH. Second, the mass flux associated with the summer (i.e., boreal winter) circulation in the SH is larger than that in the NH. The latter is attributable to the mean zonal wind, which is westerly up to 30 hPa at the middle- and high-latitude regions of the SH, satisfying the condition of possible upward propagation of planetary waves even in the summer season. These features are commonly seen for all reanalysis data.

The sum of RWs and zonal wind tendency roughly explains the total mass flux. The contribution of the zonal wind tendency is large in the autumn of each hemisphere, which is consistent with the characteristic structure of $\Psi_{dU/dt}(\phi, z)$, as discussed in section 3.3.

The percentage of the GW contribution to the mass flux largely depends on the reanalysis data. The contribution of the GWs to the mass flux is ~20 % at 70 hPa for MERRA and MERRA-2 at the most, while it is ~35–40 % for ERA-Interim and JRA-55. However, there are common interesting characteristics: The GW contribution is positive in most months and maximized in March (i.e., spring) for the NH and in July (i.e., winter) for the SH, although the estimate in June for JRA-55 could not be made because the turn-around latitude is lower than 20° in the SH.

Figure 11 shows the results for 10 hPa. Estimates at this level could not be made for several months in the SH for ERA-Interim and JRA-55 data because the turn-around latitude is lower than 20°. The total upward mass flux has a strong peak in December and January and a weak peak in October. These peaks reflect strong RW activity in each hemisphere. The SH contribution to the upward mass flux in the boreal winter is almost zero unlike that at 70 hPa as is consistent with mean easterly wind at this level. The contribution by GWs at 10 hPa is smaller than that at 70 hPa. According to the results by MERRA-2 and MERRA data, the annual mean contribution is less than 5 %. The GW contribution is largely positive for October, but there is no systematic bias in its sign in the other month. This small GW contribution elucidated by this analysis is interesting because the GW forcing largely modifies the turn-around latitudes even at 10 hPa, as shown in Section 3.1.

The upward mass flux and its contribution by each hemisphere is shown in Fig.12 as a function of the pressure level. As stated, the annual variation with a maximum in the boreal winter is dominant in the lower stratosphere, while clear semi-annual variation is observed in the upper stratosphere. The second maximum is observed earlier at the higher altitudes in the austral winter and/or spring above the 10 hPa level, which is attributed to the SH circulation.

5. Seasonal variation of the potential GW contribution and its relation with the GW activity

The $\Psi_{GW}(\phi, z)$ is equatorward in the low-latitude region and poleward in the middle-latitude region in all seasons, although the strength and vertical extension differ and depend on the reanalysis data. In this section, we describe the GW contribution in terms of seasonal dependence and consistency with previous observational studies.

The poleward circulation in $\Psi_{GW}(\phi, z)$ in the middle- and high-latitude regions is strongest in winter (DJF) and second largest in autumn (SON) in the NH, while it is strong in winter (JJA) and spring (SON) with a slight difference in the strength in the SH. The maximum in winter is consistent with previous GW studies using radiosondes (Allen and Vincent, 1995; Wang and Geller, 2003) and radars (Sato, 1994). The strong spring circulation in the SH is consistent with the fact that the GW energy is maximized in spring in the high-latitude region (Pfenninger et al., 1999; Yoshiki and Sato, 2000). Note such a spring maximum is also seen at Davis in the Antarctic in Fig. 10 of Allen and Vincent (1995), although its presence was not documented. This strong GW forcing in SON in the SH may be related to the large GW contribution to the upward mass flux in October observed at 10 hPa (Fig. 11).

The equatorward circulation of Ψ_{GW} in the low-latitude region is strong in summer and weak in winter for both hemispheres (Figs. 6 and 7). This is consistent with radiosonde observations by Allen and Vincent (1995) and rocketsonde observations by Eckermann et al. (1995) for subtropical regions, and a GW-resolving general circulation model (Sato et al., 2009). Interestingly, the equinoctial seasons, the equatorward circulation is strong in SON than in MAM for both hemispheres, similar to the poleward circulation in the middle- and high-latitude regions. This feature should be confirmed by observations because the GW characteristics in equinoctial seasons have not been studied in depth thus far.

It is also worth noting that GW activity in the equatorial stratosphere is largely modulated by the quasi-biennial oscillation (Alexander and Vincent, 2000; Sato and Dunkerton, 1997) and does not show clear seasonal variation. This feature cannot be examined in this study because f (or $\hat{f}$) in the denominator of Eqs. (7) and (9) is used for the estimation.

6. Summary and concluding remarks

The climatology of the residual mean circulation in the whole stratosphere, which is a main component of BDC, has been examined by using four reanalysis datasets (MERRA-2, MERRA, ERA-Interim, and JRA-55) over 30 years (1986–2015) based on the TEM primitive equation. One purpose of this study is to elucidate the role of GWs in the residual mean circulation, and the other is to describe the circulation in the middle and upper stratosphere, which is available with the aid of the recent reanalysis covering the upper stratosphere and the lower mesosphere. An analysis was focused on the stream function of the residual mean circulation and the upward mass flux at 70 hPa and 10 hPa evaluated from the stream function.

The stream function of the total residual mean circulation was divided into three components, namely, due to the RW forcing, the GW forcing, and the zonal mean zonal wind tendency, according to the zonal mean zonal momentum equation. The former two components were examined as potential RW and GW contributions, and the latter as a potential radiative contribution. The total residual mean stream function was directly estimated by its definition. The GW potential contribution

was estimated as the residual of the RW and radiation contributions from the total residual mean stream function. Vertical advection of the zonal mean zonal wind is also included for the analysis because the GW forcing may be small and comparable to this term in the stratosphere.

5 The annual mean total residual circulation is approximately symmetric around the equator and is composed of an equator-to-pole circulation in each hemisphere. The total residual circulation is determined by the RW forcing, as is well known. However, the contribution of GWs is also significant. The circulation by GWs is equatorward in the low-latitude region and poleward in the middle- and high-latitude regions, which correspond to eastward and westward forcings, respectively. This GW-induced circulation determines the turn-around latitudes of the total circulation at each height and extends the total circulation to high latitudes in the middle and upper stratosphere. This is one of the new and important findings elucidated by
10 this study. Similar GW contributions are observed in all seasons.

  The total circulation in the equinoctial seasons is interesting. The structure is not symmetric around the equator, but wider in autumn than in spring. This asymmetry is attributable to the radiative-driven circulation from the spring pole to the autumn pole corresponding to the zonal mean zonal wind tendency, which is understood by the angular momentum conservation. In contrast, the RW and GW contributions are almost symmetric around the equator. The direction of the
15 radiative circulation is the same as that of potential RW and GW circulations in autumn but is opposite in spring, except for the GW one in the low-latitude region.

  The potential GW contribution exhibits interesting seasonal variation, which is maximized in slightly different seasons between the NH and SH. The maximum is observed in winter in both hemispheres, but the second maximum is observed in autumn in NH and in spring in SH. This means that the GW contribution is stronger in SON than in MAM globally.
20 It is interesting to confirm this feature by analyzing GWs using high-resolution satellite observations.

  The upward mass flux exhibits annual variation with a maximum in the boreal winter in the lower stratosphere, while it is maximized twice in a year in the middle and upper stratosphere. The former is explained not only by strong RW activity in winter NH but also by strong RW activity in summer SH. The GW contribution to the upward mass flux is not very large, at approximately 10–40 % at 70 hPa and less than 5 % at 10 hPa depending on the reanalysis data, although the estimation for
25 10 hPa was not made for ERA-Interim and JRA-55. This small GW contribution to the upward mass flux is interesting, as the GWs are essential to determine the turn-around latitude.

  The features on the GW contributions to the stream function of the residual mean circulation described above are commonly observed for all reanalysis data, suggesting that they are robust results. In contrast, a significant difference among the reanalysis was observed in the percentage of the GW contributions to the upward mass flux. One conceivable cause is that
30 the GW contribution is relatively small at the turn-around latitude, although the turn-around latitude itself is largely affected by GWs. Another one is the difference in the GW parameterization schemes used in the model for each reanalysis, which suggests the inadequateness of the GW parameterizations. For example, most GW parameterizations produce the latitudinal distribution of momentum fluxes, which does not accord with observations particularly at high latitudes (Geller et al., 2013). In addition, they assume only vertical propagation, although the horizontal propagation of GWs by refraction, advection, and

their own horizontal group velocity is sometimes significant (e.g., Sato et al., 2009, 2012). BDC affects the global climate by modifying the tropopause structure, such as static stability and westerly jet latitudes (e.g., Kidston et al., 2015; Kohma and Sato, 2014; Li and Thompson, 2013). The significant potential contribution of GWs shown by the present study indicates the necessity of further constraint to the GW parameterization by high-resolution observations. The use of GW permitting general
5 circulation models is also promising.

Acknowledgements

This study was an extensive study initiated by a part of Kota Okamoto's PhD thesis, for which KS supervised. The authors thank Yoshihiro Tomikawa, Takenari Kinoshita, and Masashi Kohma for their fruitful discussion. This study was supported by the Sumitomo Foundation and by JSPS Kakenhi Grant Number 25247075.

10 **Appendix A: Difference in the residual mean stream function between the vertical integration of $\overline{v}^*$ and the latitudinal integration of $\overline{w}^*$**

As described in section 2, there are two methods to estimate $\Psi(\phi, z)$ from the residual mean flow: One is a vertical integration of $\overline{v}^*$ from the top, and the other is a latitudinal integration of $\overline{w}^*$ from the North Pole or the South Pole. The former scheme has an advantage in which a relatively large, and hence (probably) a reliable quantity of $\overline{v}$ can be used, but a disadvantage in
15 which $\overline{v}^*$ above the top of the data needs to be ignored. In contrast, the latter method requires the use of quite a small quantity $\overline{w}$, but an exact boundary condition, $\overline{w}^* = 0$, at the pole can be used.

Figures Aa, Ad, and Ag show the stream functions obtained from the vertical integration for the annual mean state, for DJF, and for MAM using MERRA-2 data. Figures Ab, Ae, and Ah (Ac, Af, and Ai) show those obtained using the latitudinal integration from the North (South) Pole. Note that the results of two latitudinal integrations from the North Pole
20 and from the South Pole accord at least in the low-latitude region. The difference seen in the high-latitude region of the opposite hemisphere to the initial location for the integration is likely due to the accumulation of error in $\overline{w}^*$ through the integration. The stream functions of total circulation shown in Figs. 2–12 of this paper were made by joining the NH and SH stream functions at the equator, which were obtained by the latitudinal integration from the North and South Poles, respectively.

Next, the results between the vertical and latitudinal integrations are compared. The annual mean $\Psi(\phi, z)$ obtained
25 from the vertical (Fig. Aa) and latitudinal (Fig. 2a) integrations accord well for the main part of the stratosphere, although the $\Psi(\phi, z)$ values from the vertical integration for the upper stratosphere and lower mesosphere above 5 hPa are smaller in both the NH and SH than those from the latitudinal integration. This suggests that the residual mean circulation in the lower and middle stratosphere is mainly determined by the wave forcing in the stratosphere, but the effect of the wave forcing in the mesosphere is not completely negligible for the circulation in the upper stratosphere. These features are similarly observed for
30 the equinoctial seasons (i.e., Fig. Ag and 8a for MAM).

The difference for the solstitial seasons is more complex. The $\Psi(\phi, z)$ from the vertical integration has a deeper summer circulation and a slightly weaker winter circulation than that from the latitudinal integration. This result is consistent with the existence of the GW forcing in the mesosphere that is westward in the summer hemisphere and westward in the winter hemisphere, which is ignored for the estimation from the vertical integration. In fact, the summer to winter pole circulation caused by the GW forcing that should be observed in the mesosphere is clearer in the lower most mesosphere in the $\Psi(\phi, z)$ (above 1 hPa) from the latitudinal integration (Fig. 6a).

In conclusion, the stream function of the residual mean circulation is better calculated from $\overline{w}^*$ by the latitudinal integration using recent modern reanalysis data.

Appendix B: Effects of the vertical shear of mean zonal wind on the residual mean stream function

As described by Haynes et al. (1991), the vertical integration should be made along a contour of the angular momentum (m) when the vertical advection by the residual mean flow $\overline{w}^* \frac{d\overline{u}}{dz}$ is not negligible. This may be the case for a low-latitude region where the latitudinal gradient of the angular momentum is small (i.e., f is small) [see Fig. 1 of Haynes et al. (1991), for example]. However, it is not easy to calculate the integration along the m contour. Thus, several previous studies used a simple integration in the vertical at a latitude ignoring the term $\overline{w}^* \frac{d\overline{u}}{dz}$ instead of the integration along the m contour. It is therefore useful to compare the results from the two methods and discuss the limitation of the simple vertical integration. It will be useful to discuss the limitation of this simplified method using this comparison.

As seen in Fig. 1 of Haynes et al. (1991), the m contours are greatly distorted at latitudes lower than 30° and even closed contours are observed near the equator, while they are almost vertical at higher latitudes. Figure B-1 (B-2) shows the meridional cross sections of Ψ_{RW}, $\Psi_{dU/dt}$, and Ψ_{GW} from the top obtained by the integration in the vertical at each latitude (left) and by that along the m contours (right) in DJF (JJA). As expected, a slight difference is observed in latitudes lower than 30°. A notable difference is observed in Ψ_{RW} for the low-latitude region of the SH in DJF in which the positive stream function contours are extended more poleward for the results from the along-m integration. As a result, Ψ_{GW} is slightly weaker there. Such difference is not distinct for the NH in JJA. Another difference is observed in Ψ_{GW} in the low-latitude region of the winter hemisphere around 20 hPa particularly in the SH in JJA, where a small counter circulation (i.e., equatorward) is present. This counter circulation is more evident for the along-m integration. Similarly, a slight difference was observed for the equinoctial seasons (not shown), but one of the important findings of the present paper that the equatorward circulation by GWs in the low-latitude region is stronger in SON than in MAM is robust for the different vertical integration. Therefore, it is concluded that although the vertical advection term, $\overline{w}^* \frac{d\overline{u}}{dz}$, is not negligible in the low-latitude region, overall features in the residual circulation including potential contributions by GWs can be estimated by a simple vertical integration of the wave forcing.

References

Alexander, M. J. and Vincent, R. A.: Gravity waves in the tropical lower stratosphere: An observational study of seasonal and interannual variability, J. Geophys. Res. Atmos., 105(D14), 17971–17982, doi:10.1029/2000JD900196, 2000.

Allen, S. J. and Vincent, R. A.: Gravity wave activity in the lower atmosphere: Seasonal and latitudinal variations, J. Geophys. Res., 100(D1), 1327–1350, doi:10.1029/94JD02688, 1995.

Andrews, D. G., Holton, J. R. and Leovy, C. B.: Middle Atmosphere Dynamics, Academic Press., 1987.

Birner, T. and Bönisch, H.: Residual circulation trajectories and transit times into the extratropical lowermost stratosphere, Atmos. Chem. Phys., 11(2), 817–827, doi:10.5194/acp-11-817-2011, 2011.

Butchart, N.: The Brewer-Dobson circulation, Rev. Geophys, 52, 157–184, doi:10.1002/2013RG000448, 2014.

Butchart, N., Cionni, I., Eyring, V., Shepherd, T. G., Waugh, D. W., Akiyoshi, H., Austin, J., Brühl, C., Chipperfield, M. P., Cordero, E., Dameris, M., Deckert, R., Dhomse, S., Frith, S. M., Garcia, R. R., Gettelman, A., Giorgetta, M. A., Kinnison, D. E., Li, F., Mancini, E., Mclandress, C., Pawson, S., Pitari, G., Plummer, D. A., Rozanov, E., Sassi, F., Scinocca, J. F., Shibata, K., Steil, B. and Tian, W.: Chemistry-climate model simulations of twenty-first century stratospheric climate and circulation changes, J. Clim., 23(20), 5349–5374, doi:10.1175/2010JCLI3404.1, 2010.

Charney, J. G. and Drazin, P. G.: Propagation of planetary-scale disturbances from the lower into the upper atmosphere, J. Geophys. Res., 66(1), 83–109, doi:10.1029/JZ066i001p00083, 1961.

Chun, H.-Y., Kim, Y.-H., Choi, H.-J. and Kim, J.-Y.: Influence of Gravity Waves in the Tropical Upwelling: WACCM Simulations, J. Atmos. Sci., 68(11), 2599–2612, doi:10.1175/JAS-D-11-022.1, 2011.

Cohen, N. Y., Gerber, E. P. and Bühler, O.: Compensation between Resolved and Unresolved Wave Driving in the Stratosphere: Implications for Downward Control, J. Atmos. Sci., 70(12), 3780–3798, doi:10.1175/JAS-D-12-0346.1, 2013.

Dee, D. P., Uppala, S. M., Simmons, A. J., Berrisford, P., Poli, P., Kobayashi, S., Andrae, U., Balmaseda, M. A., Balsamo, G., Bauer, P., Bechtold, P., Beljaars, A. C. M., van de Berg, L., Bidlot, J., Bormann, N., Delsol, C., Dragani, R., Fuentes, M., Geer, A. J., Haimberger, L., Healy, S. B., Hersbach, H., Hólm, E. V., Isaksen, L., Kållberg, P., Köhler, M., Matricardi, M., Mcnally, A. P., Monge-Sanz, B. M., Morcrette, J. J., Park, B. K., Peubey, C., de Rosnay, P., Tavolato, C., Thépaut, J. N. and Vitart, F.: The ERA-Interim reanalysis: Configuration and performance of the data assimilation system, Q. J. R. Meteorol. Soc., 137(656), 553–597, doi:10.1002/qj.828, 2011.

Dunkerton, T. J.: Nonlinear Hadley circulation driven by asymmetric differential heating, J. Atmos. Sci., 46(7), 956–974, 1989.

Eckermann, S. D., Hirota, I. and Hocking, W. K.: Gravity wave and equatorial wave morphology of the stratosphere derived from long-term rocket soundings, Q. J. R. Meteorol. Soc., 121(521), 149–186, doi:10.1002/qj.49712152108, 1995.

Fujiwara, M., Wright, J. S., Manney, G. L., Gray, L. J., Anstey, J., Birner, T., Davis, S., Gerber, E. P., Harvey, V. L., Hegglin, M. I., Homeyer, C. R., Knox, J. A., Kruger, K., Lambert, A., Long, C. S., Martineau, P., Molod, A., Monge-Sanz, B. M., Santee, M. L., Tegtmeier, S., Chabrillat, S., Tan, D. G. H., Jackson, D. R., Polavarapu, S., Compo, G. P., Dragani, R.,

Ebisuzaki, W., Harada, Y., Kobayashi, C., McCarty, W., Onogi, K., Pawson, S., Simmons, A., Wargan, K., Whitaker, J. S. and Zou, C.-Z.: Introduction to the SPARC Reanalysis Intercomparison Project (S-RIP) and overview of the reanalysis systems, Atmos. Chem. Phys., 17(2), 1417–1452, doi:10.5194/acp-17-1417-2017, 2017.

Garcia, R. R.: On the Mean Meridional Circulation of the Middle Atmosphere, J. Atmos. Sci., 44(24), 3599–3609, doi:10.1175/1520-0469(1987)044<3599:OTMMCO>2.0.CO;2, 1987.

Gelaro, R., McCarty, W., Suárez, M. J., Todling, R., Molod, A., Takacs, L., Randles, C. A., Darmenov, A., Bosilovich, M. G., Reichle, R., Wargan, K., Coy, L., Cullather, R., Draper, C., Akella, S., Buchard, V., Conaty, A., da Silva, A. M., Gu, W., Kim, G. K., Koster, R., Lucchesi, R., Merkova, D., Nielsen, J. E., Partyka, G., Pawson, S., Putman, W., Rienecker, M., Schubert, S. D., Sienkiewicz, M. and Zhao, B.: The modern-era retrospective analysis for research and applications, version 2 (MERRA-2), J. Clim., 30(14), 5419–5454, doi:10.1175/JCLI-D-16-0758.1, 2017.

Geller, M. A., Alexander, J. J., Love, P. T., Bacmeister, J., Ern, M., Hertzog, A., Manzini, E., Preusse, P., Sato, K., Scaife, A. A. and Zhou, T.: A comparison between gravity wave momentum fluxes in observations and climate models, J. Clim., 26(17), 6383–6405, doi:10.1175/JCLI-D-12-00545.1, 2013.

Hayashi, Y. and Sato, K.: Formation of two-dimensional circulation in response to unsteady wave forcing in the middle atmosphere, J. Atmos. Sci., 75, 125–142, doi:10.1175/JAS-D-16-0374.1, 2018.

Haynes, P. H., McIntyre, M. E., Shepherd, T. G., Marks, C. J. and Shine, K. P.: On the "Downward Control" of Extratropical Diabatic Circulations by Eddy-Induced Mean Zonal Forces, J. Atmos. Sci., 48(4), 651–678, doi:10.1175/1520-0469(1991)048<0651:OTCOED>2.0.CO;2, 1991.

Hertzog, A., Boccara, G., Vincent, R. A., Vial, F. and Cocquerez, P.: Estimation of Gravity Wave Momentum Flux and Phase Speeds from Quasi-Lagrangian Stratospheric Balloon Flights. Part II: Results from the Vorcore Campaign in Antarctica, J. Atmos. Sci., 65(10), 3056–3070, doi:10.1175/2008JAS2710.1, 2008.

Kerr-Munslow, A. M. and Norton, W. A.: Tropical Wave Driving of the Annual Cycle in Tropical Tropopause Temperatures. Part I: ECMWF Analyses, J. Atmos. Sci., 63(5), 1410–1419, doi:10.1175/JAS3698.1, 2006.

Kidston, J., Scaife, A. A., Hardiman, S. C., Mitchell, D. M., Butchart, N., Baldwin, M. P. and Gray, L. J.: Stratospheric influence on tropospheric jet streams, storm tracks and surface weather, Nat. Geosci., 8(6), 433–440, doi:10.1038/NGEO2424, 2015.

Kitamura, Y. and Hirota, I.: Small-scale Disturbances in the Lower Stratosphere Revealed by Daily Rawin Sonde Observation, Journat Meterotogical Soc. Japan, 67(5), 817–831, 1989.

Kobayashi, S., Ota, Y., Harada, Y., Ebita, A., Moriya, M., Onoda, H., Onogi, K., Kamahori, H., Kobayashi, C., Endo, H., Miyaoka, K. and Takahashi, K.: The JRA-55 Reanalysis: General Specifications and Basic Characteristics, J. Meteorol. Soc. Japan. Ser. II, 93(1), 5–48, doi:10.2151/jmsj.2015-001, 2015.

Kohma, M. and Sato, K.: Variability of upper tropospheric clouds in the polar region during stratospheric sudden warmings, J. Geophys. Res. Atmos., 119, 10100–10113, doi:10.1002/2014JD021746., 2014.

Li, Y. and Thompson, D. W. J.: The signature of the stratospheric Brewer-Dobson circulation in tropospheric clouds, J. Geophys. Res. Atmos., 118(9), 3486–3494, doi:10.1002/jgrd.503392013, 2013.

Lilly, D. K. and Kennedy, P. J.: Observations of a Stationary Mountain Wave and its Associated Momentum Flux and Energy Dissipation, J. Atmos. Sci., 30(September), 1135–1152, doi:10.1175/1520-

5   0469(1973)030<1135:OOASMW>2.0.CO;2, 1973.

McLandress, C. and Shepherd, T. G.: Simulated anthropogenic changes in the Brewer-Dobson circulation, including its extension to high latitudes, J. Clim., 22(6), 1516–1540, doi:10.1175/2008JCLI2679.1, 2009.

Norton, W. A.: Tropical Wave Driving of the Annual Cycle in Tropical Tropopause Temperatures. Part II: Model Results, J. Atmos. Sci., 63(5), 1420–1431, doi:10.1175/JAS3698.1, 2006.

10   Okamoto, K., Sato, K. and Akiyoshi, H.: A study on the formation and trend of the Brewer-Dobson circulation, J. Geophys. Res. Atmos., 116(10), 1–11, doi:10.1029/2010JD014953, 2011.

Pfenninger, M., Liu, A. Z., Papen, G. C. and Gardner, C. S.: Gravity wave characteristics in the lower atmosphere at south pole, J. Geophys. Res., 104(D6), 5963, doi:10.1029/98JD02705, 1999.

Pfister, L., Chan, K., Bui, T. P., Bowen, S., Legg, M., Gary, B., Kelly, K., Proffitt, M. and Starr, W.: Gravity waves

15   generated by a tropical cyclone during the STEP tropical field program- A case study, J. Geophys. Res., 98(D5), 8611–8638, doi:10.1029/92JD01679, 1993.

Plumb, R.: Stratospheric Transport., J. Meteorol. Soc. Japan, 80(4B), 793–809, doi:10.2151/jmsj.80.793, 2002.

Randel, W. J., Garcia, R. R. and Wu, F.: Time-Dependent Upwelling in the Tropical Lower Stratosphere Estimated from the Zonal-Mean Momentum Budget, J. Atmos. Sci., 59(13), 2141–2152, doi:10.1175/1520-

20   0469(2002)059<2141:TDUITT>2.0.CO;2, 2002.

Randel, W. J., Garcia, R. and Wu, F.: Dynamical Balances and Tropical Stratospheric Upwelling, J. Atmos. Sci., 65(11), 3584–3595, doi:10.1175/2008JAS2756.1, 2008.

Rienecker, M. M., Suarez, M. J., Gelaro, R., Todling, R., Bacmeister, J., Liu, E., Bosilovich, M. G., Schubert, S. D., Takacs, L., Kim, G. K., Bloom, S., Chen, J., Collins, D., Conaty, A., Da Silva, A., Gu, W., Joiner, J., Koster, R. D., Lucchesi, R.,

25   Molod, A., Owens, T., Pawson, S., Pegion, P., Redder, C. R., Reichle, R., Robertson, F. R., Ruddick, A. G., Sienkiewicz, M. and Woollen, J.: MERRA: NASA's modern-era retrospective analysis for research and applications, J. Clim., 24(14), 3624–3648, doi:10.1175/JCLI-D-11-00015.1, 2011.

Sato, K.: Vertical wind disturbances in the troposphere and lower stratosphere observed by the MU radar, J. Atmos. Sci., 47(23), 1990.

30   Sato, K.: A statistical study of the structure, saturation and sources of inertio-gravity waves in the lower stratosphere observed with the MU radar, J. Atmos. Terr. Phys., 56(6), 755–774, doi:10.1016/0021-9169(94)90131-7, 1994.

Sato, K. and Dunkerton, T. J.: Estimates of momentum flux associated with equatorial Kelvin and gravity waves, J. Geophys. Res. Atmos., 102(22), 1997.

Sato, K., Watanabe, S., Kawatani, Y., Tomikawa, Y., Miyazaki, K. and Takahashi, M.: On the origins of mesospheric gravity waves, Geophys. Res. Lett., 36(19), 1–5, doi:10.1029/2009GL039908, 2009.

Sato, K., Tateno, S., Watanabe, S. and Kawatani, Y.: Gravity Wave Characteristics in the Southern Hemisphere Revealed by a High-Resolution Middle-Atmosphere General Circulation Model., J. Atmos. Sci., 69(4), 1378–1396, doi:10.1175/JAS-D-
5   11-0101.1, 2012.

Semeniuk, K. and Shepherd, T. G.: The Middle-Atmosphere Hadley Circulation and Equatorial Inertial Adjustment, J. Atmos. Sci., 58, 3077–3096, doi:10.1175/1520-0469(2001)058<3077:TMAHCA>2.0.CO;2, 2001.

Seviour, W. J. M., Butchart, N. and Hardiman, S. C.: The Brewer-Dobson circulation inferred from ERA-Interim, Q. J. R. Meteorol. Soc., 138(665), 878–888, doi:10.1002/qj.966, 2012.

10   Shibuya, R., Sato, K., Tomikawa, Y., Tsutsumi, M. and Sato, T.: A Study of Multiple Tropopause Structures Caused by Inertia–Gravity Waves in the Antarctic, J. Atmos. Sci., 72(5), 2109–2130, doi:10.1175/JAS-D-14-0228.1, 2015.

Tanaka, H.: A Slowly Varying Model of the Lower Stratospheric Zonal Wind Minimum Induced by Mesoscale Mountain Wave Breakdown, J . Atmos. Sci, 43, 1881–1892, doi:https://doi.org/10.1175/1520-0469(1986)043<1881:ASVMOT>2.0.CO;2, 1986.

15   Wang, L. and Geller, M. A.: Morphology of gravity-wave energy as observed from 4 years (1998–2001) of high vertical resolution U.S. radiosonde data, J. Geophys. Res., 108(D16), ACL 1-1-ACL 1-12, doi:10.1029/2002JD002786, 2003.

Yoshiki, M. and Sato, K.: A statistical study of gravity waves in the polar regions based on operational radiosonde data, J. Geophys. Res. Atmos., 105(D14), 2000.
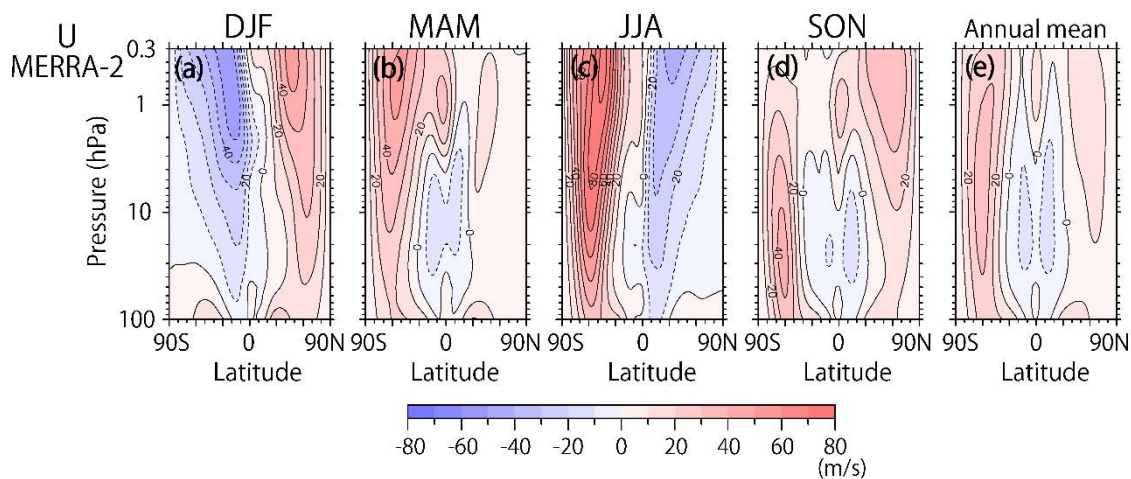
Figure 1: Meridional cross sections for the climatology of seasonal mean zonal mean zonal wind for (a) DJF, (b) MAM, (c) JJA, and (d) SON, and (e) for the annual mean.
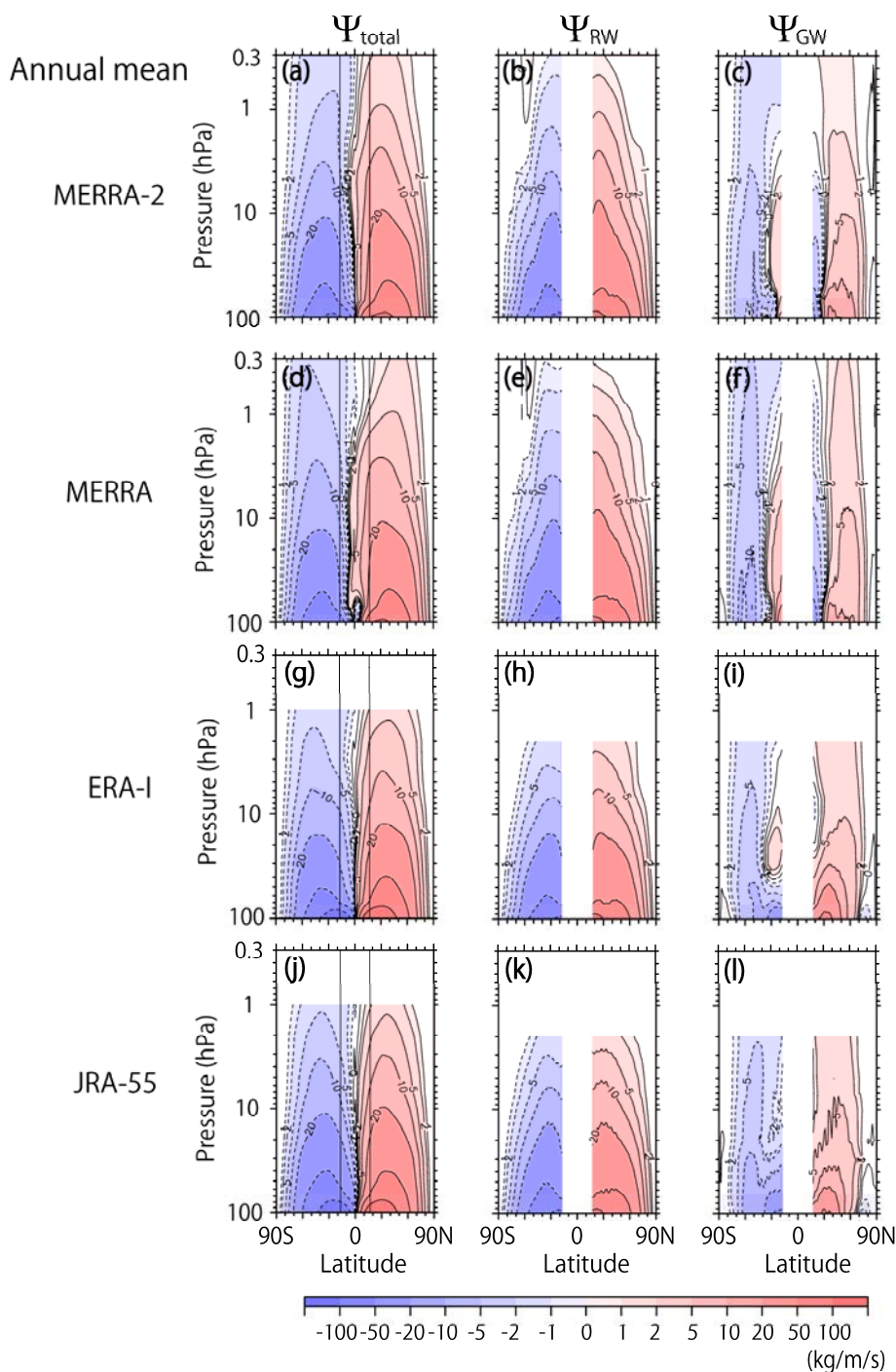
Figure 2: Meridional cross sections of the climatology of the annual mean stream function of the residual mean flow (a), contributions of RWs (resolved waves) (b) and GWs (unresolved waves) (c) for MERRA-2, for MERRA [(d), (e), and (f)], for ERA-Interim [(g), (h), and (i)], and for JRA-55 [(j), (k), and (l)].
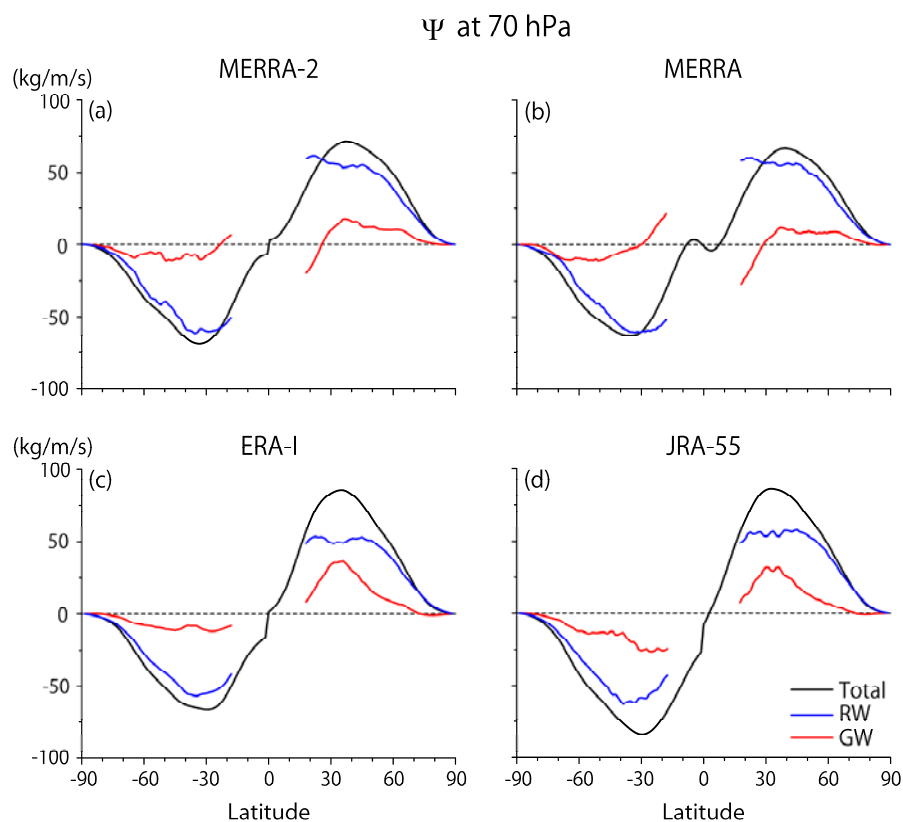
Figure 3: Latitudinal profiles of the climatology of the annual mean stream function of the residual mean flow (black), contributions of RWs (blue) and GWs (red) at 70 hPa for (a) MERRA-2, (b) MERRA, (c) ERA-Interim, and (d) JRA-55.
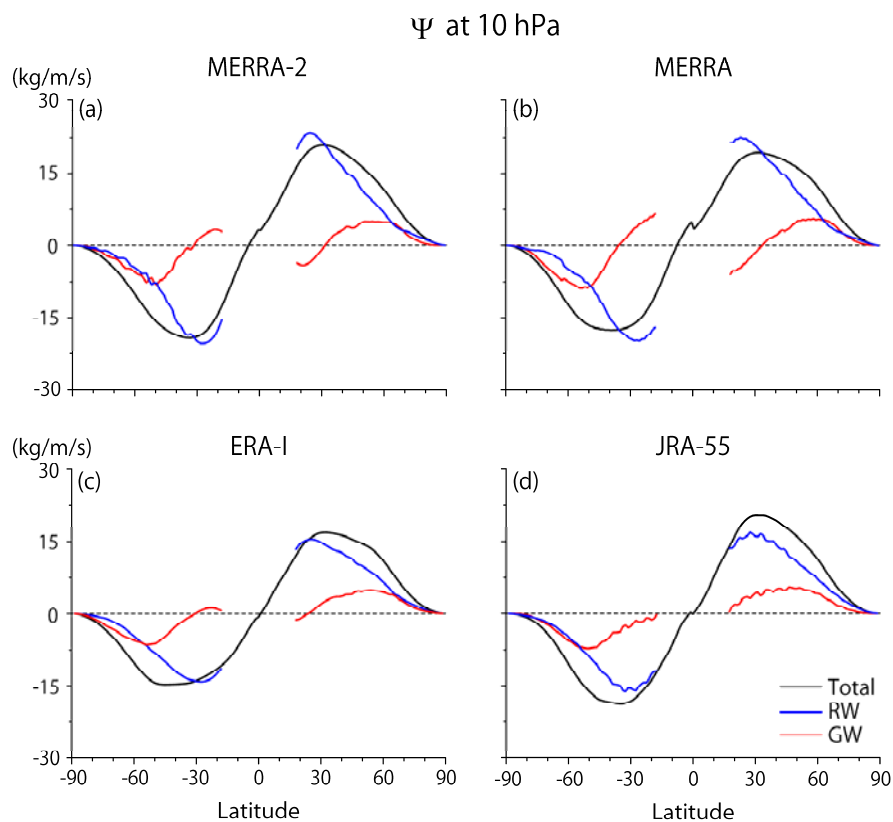
Figure 4: The same as Figure 3 but for 10 hPa.
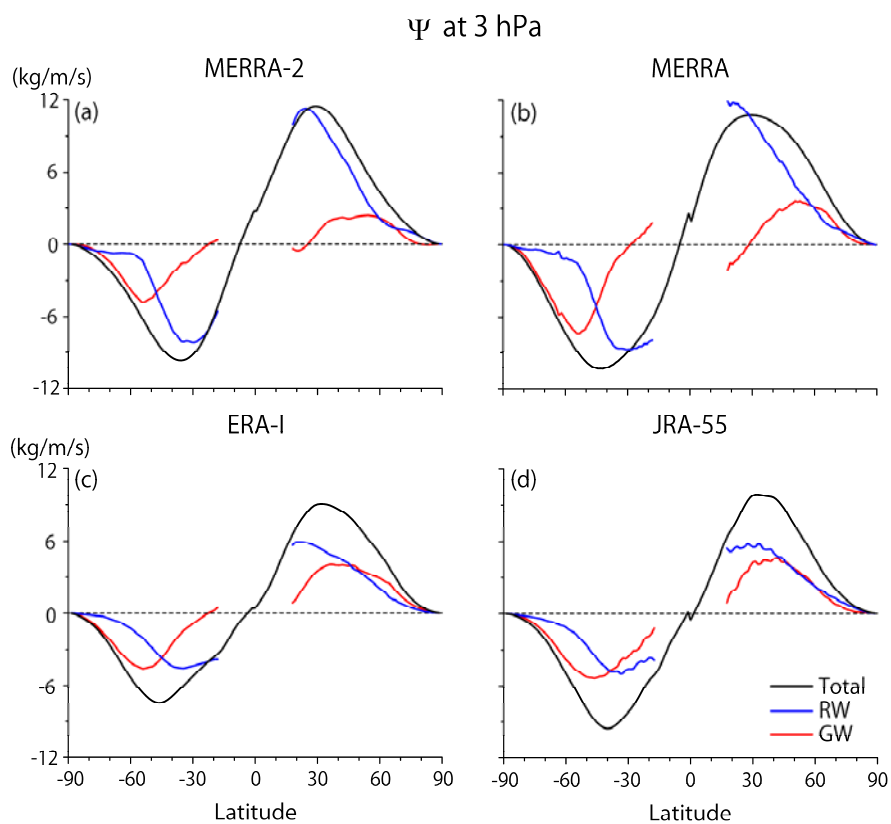
Figure 5: The same as Figure 3 but for 3 hPa.
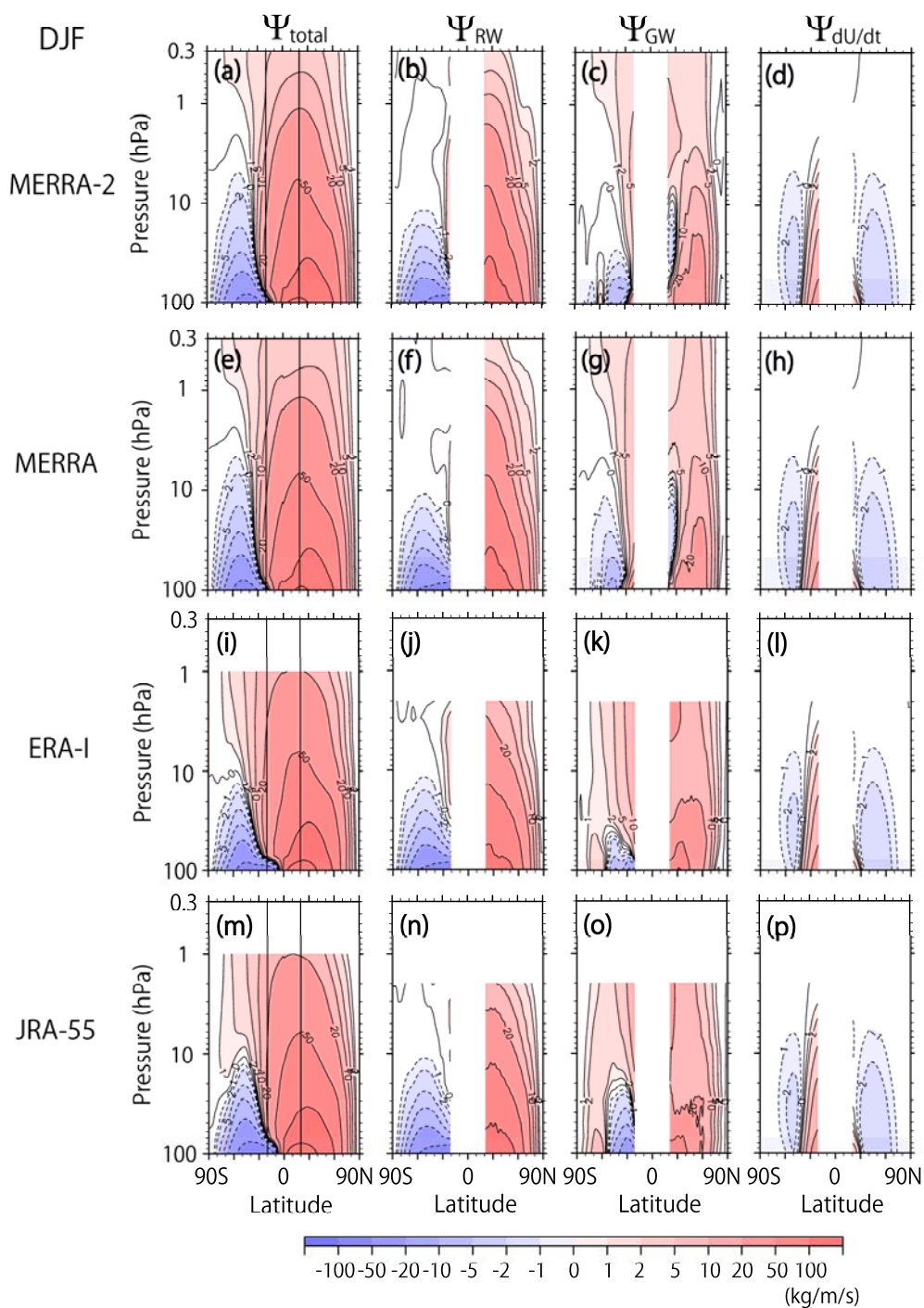
Figure 6: Meridional cross sections of the climatology of the seasonal mean stream function of the residual mean flow and potential contributions of RWs (resolved waves), GWs (unresolved waves), and the tendency of zonal mean zonal wind in DJF for MERRA-2 [from the left, (a), (b), (c), and (d)], MERRA [(e), (f), (g), and (h)], ERA-Interim [(i), (j), (k), and (l)], and JRA-55 [(i), (j), (k), and (l)].
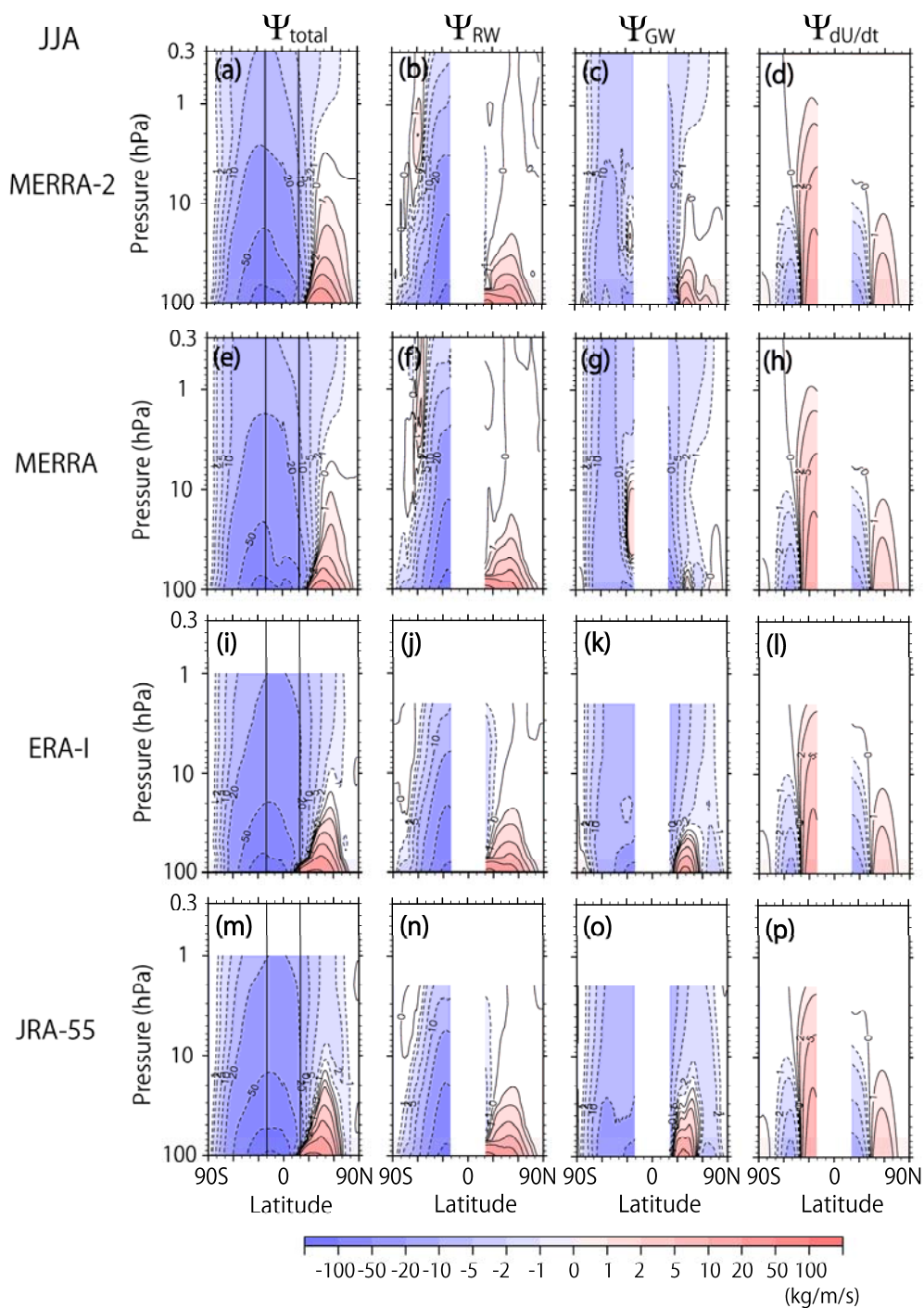
Figure 7: The same as Figure 6 but for JJA.
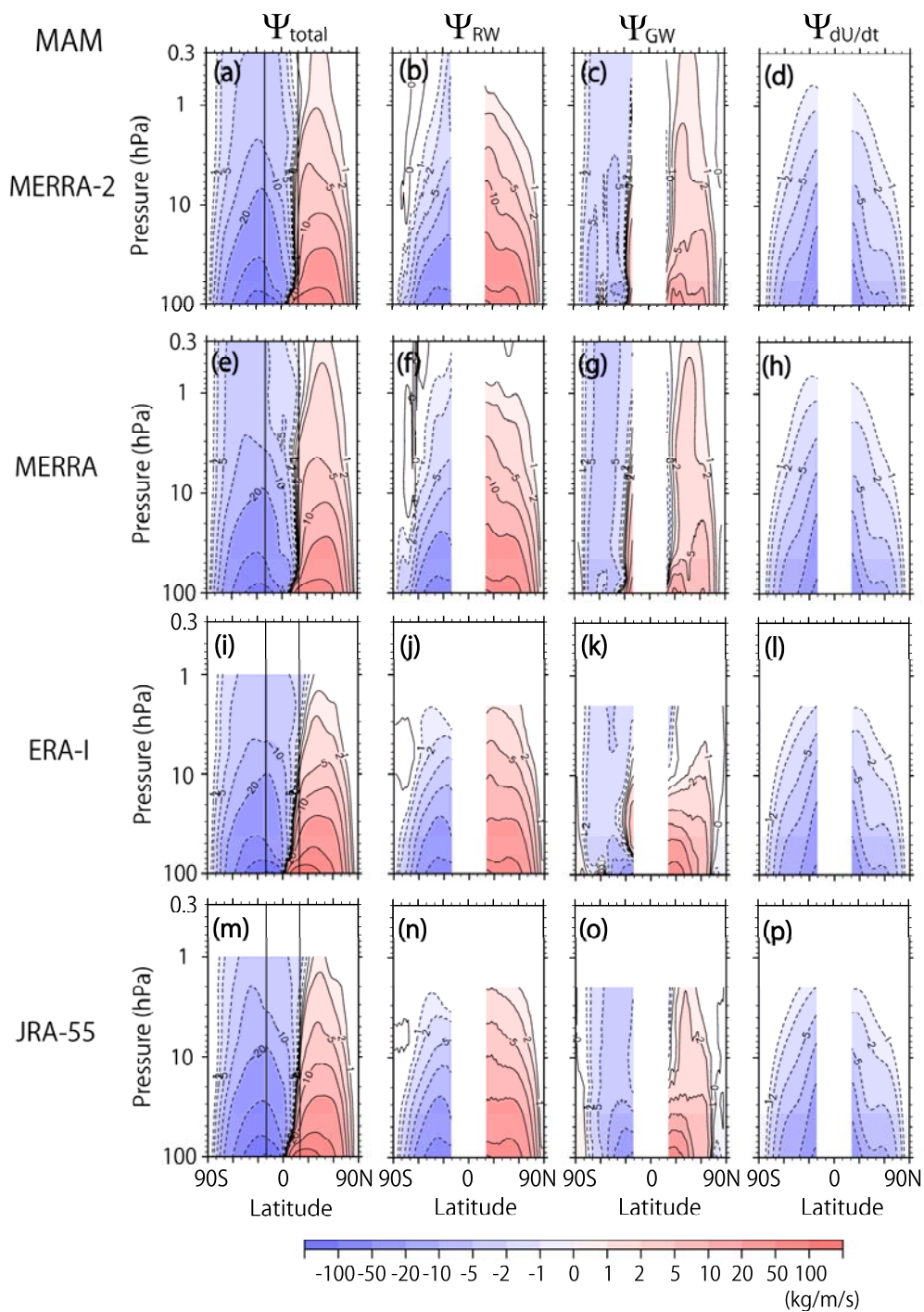
Figure 8: The same as Figure 6 but for MAM.
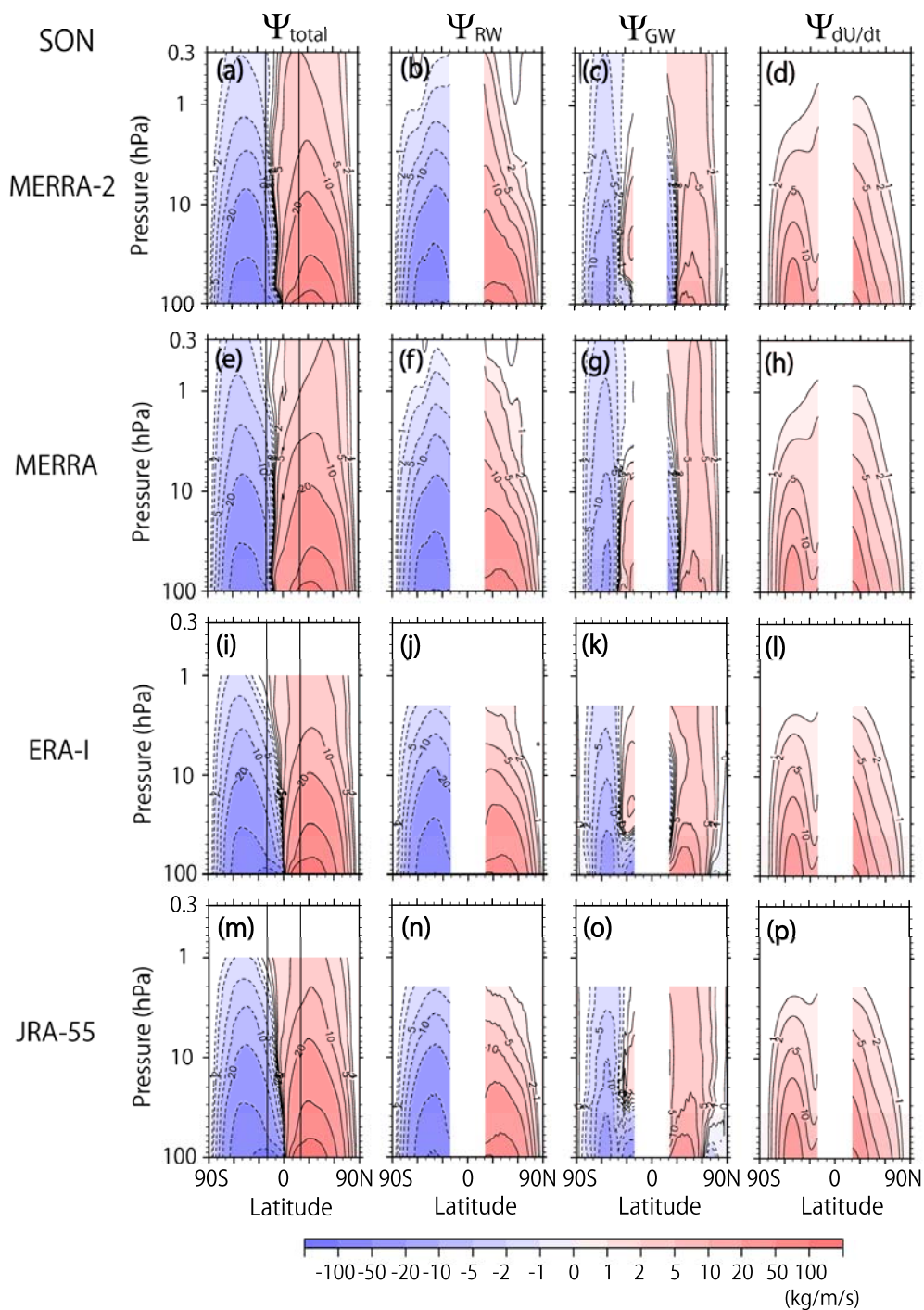
Figure 9: The same as Figure 6 but for SON.
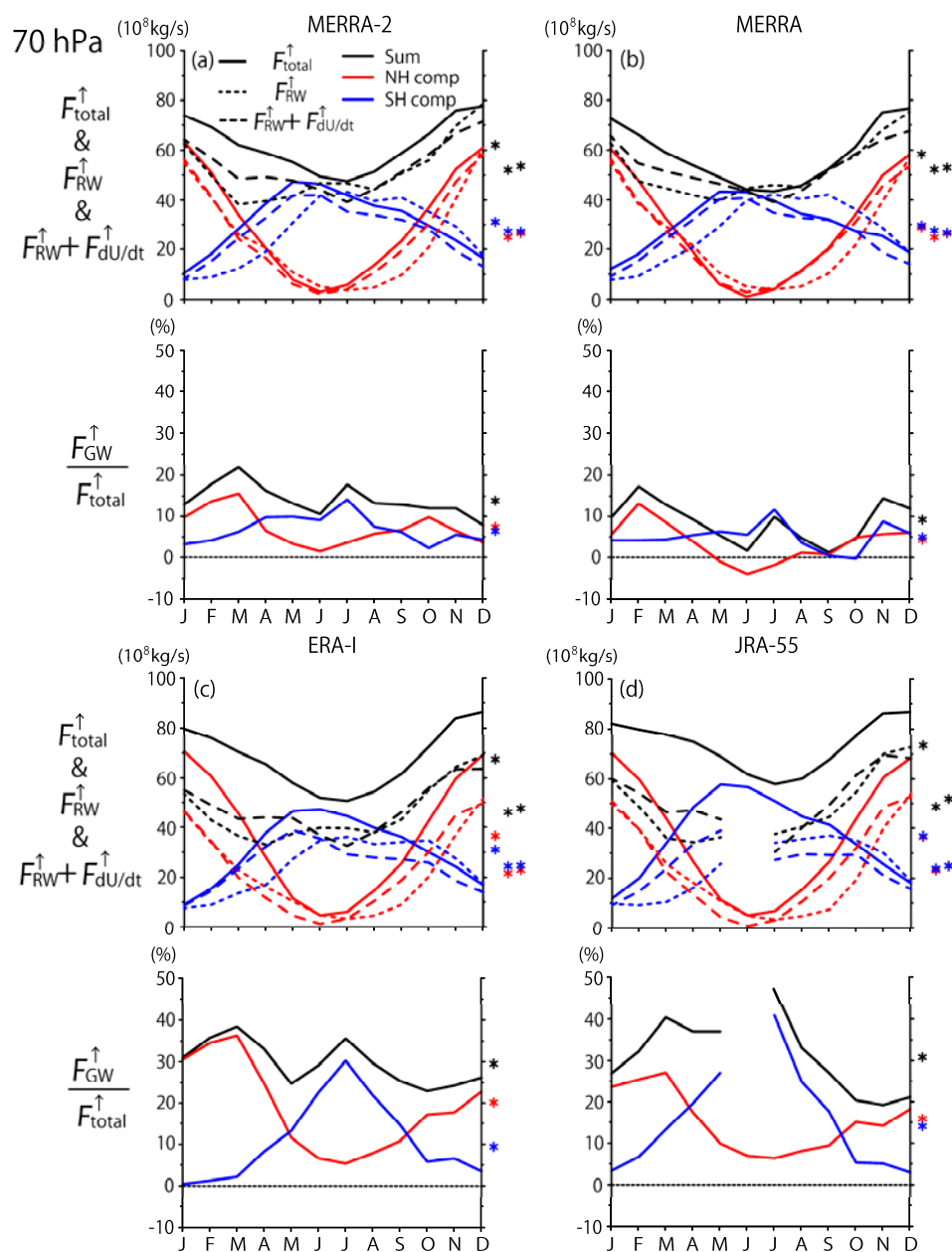
Figure 10: Upward mass flux at 70 hPa as a function of the month for (a) MERRA-2, (b) MERRA, (c) ERA-Interim, and (d) JRA-55. Upper panel: Black solid curves show the net upward mass flux and red (blue) solid curves show contributions of the NH and SH. Solid curves show the total mass flux. Dashed curves show potential contributions of Rossby waves plus the tendency of the zonal mean zonal wind. Left (right) asterisks on the right show their annual mean (the potential contributions of RWs plus the tendency of the zonal mean zonal wind. Lower panel: Percentage of the potential contribution of GWs to the total mass flux. The asterisks on the right show their annual mean.
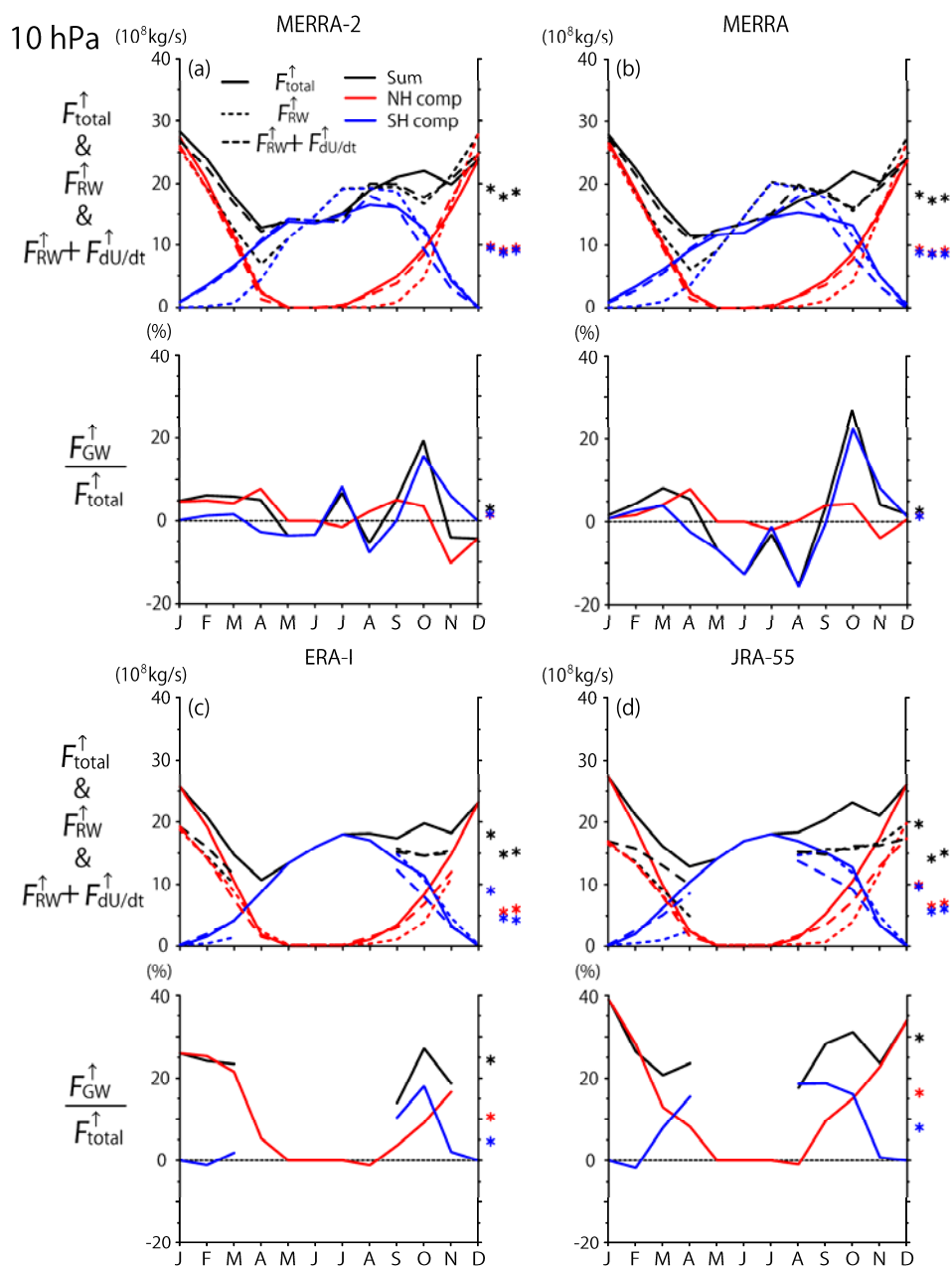
Figure 11: The same as Figure 10 but for 10 hPa.
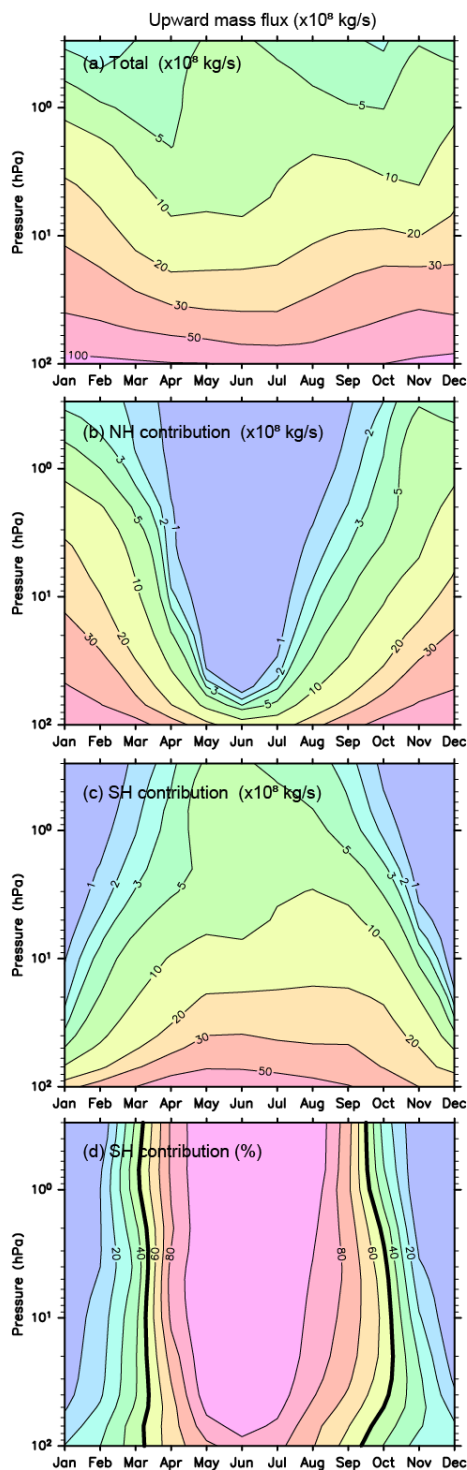
Figure 12. Upward mass flux as a function of the pressure level. (a) Total and contributions of the (b) NH and (c) SH. (d) The percentage of the SH contribution to the total upward mass flux.
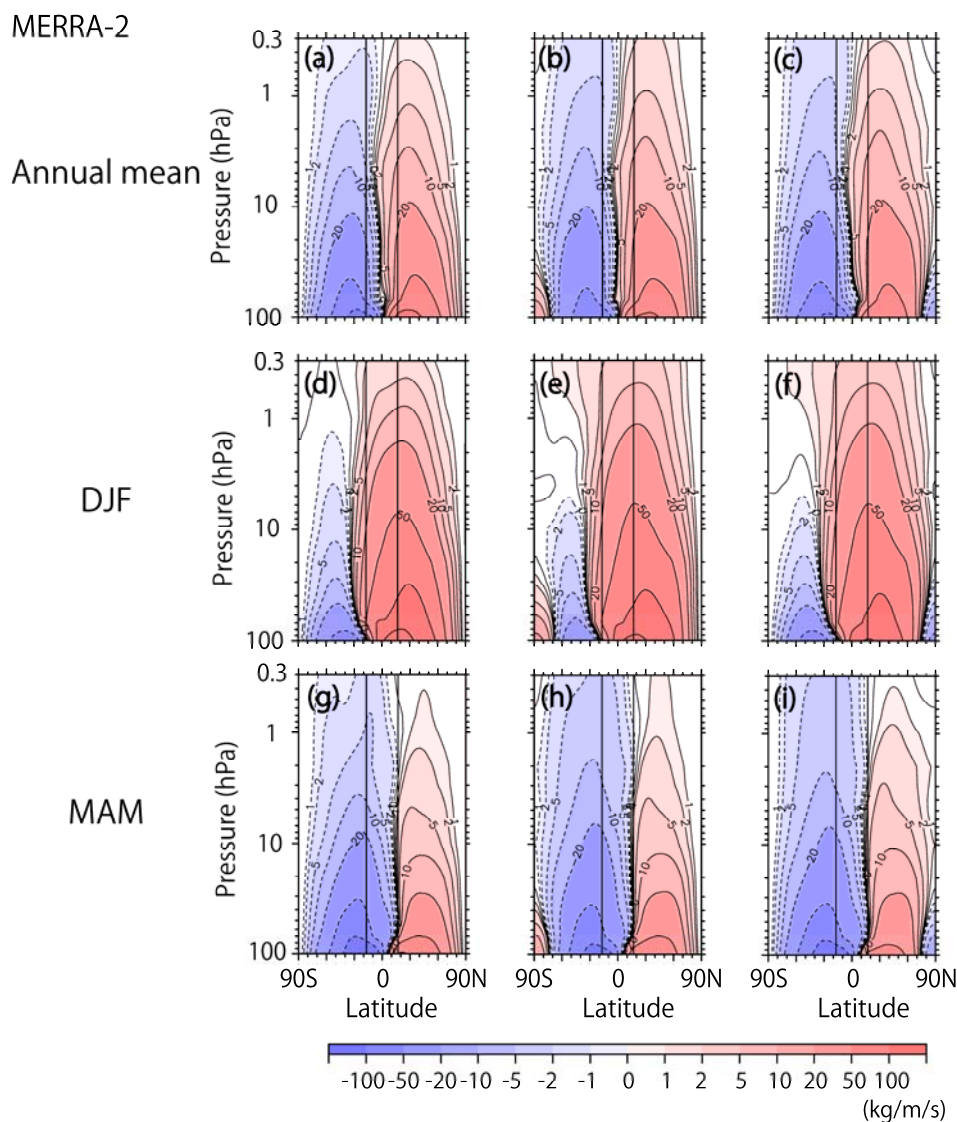
Figure A-1. Meridional cross sections of the climatology of the annual mean, DJF, and MAM stream function of the residual mean flow from the top. (a), (d), and (g): Estimates from the vertical integration of $\bar{v}^*$ [(b), (e) and (h) [(c), (f) and (i)]: Estimates from the latitudinal integration of $\bar{w}^*$ starting from the north [south] pole.
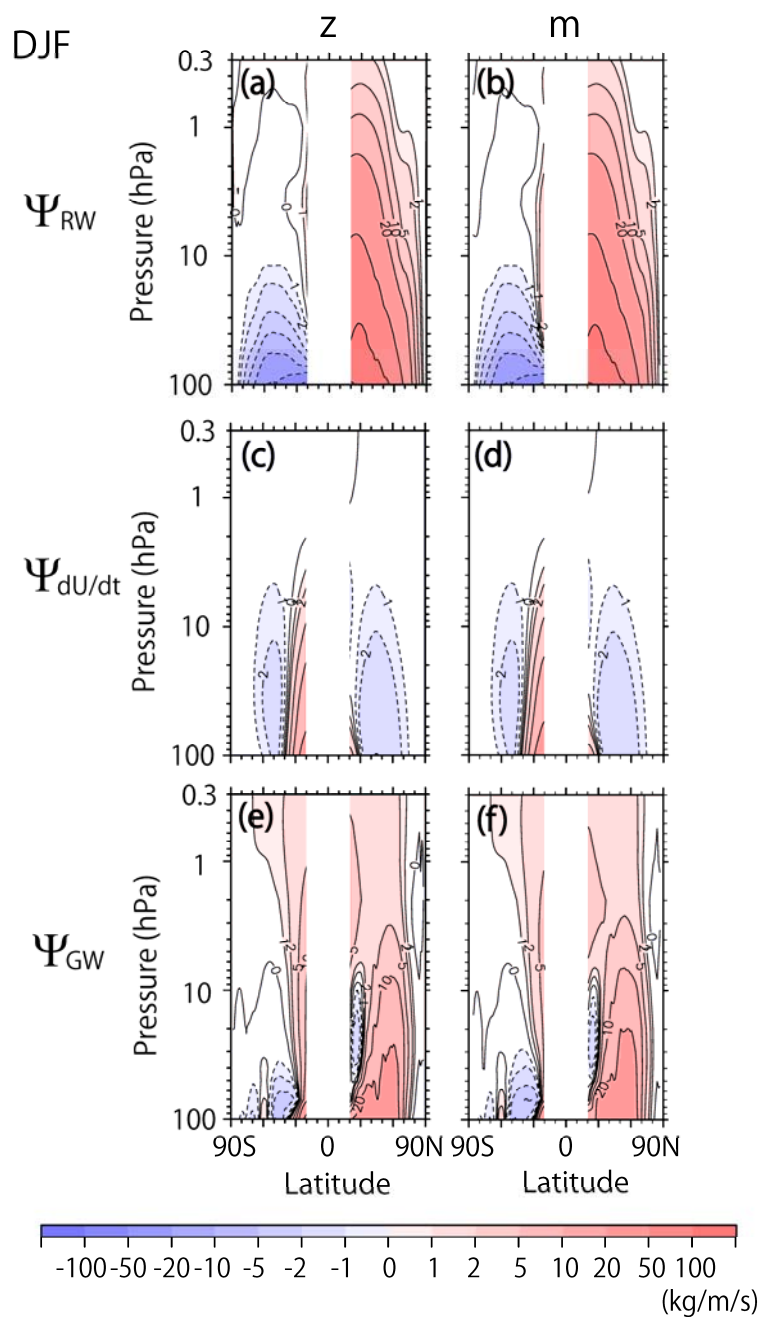
Figure B-1. Meridional cross sections of the DJF climatology of potential contributions by (a) (b) the RWs, (c) (d) the tendency of zonal mean zonal wind, and (e) (f) the GWs in DJF estimated from MERRA-2. Estimates from (a), (c), (e) a vertical integral at a constant latitude (i.e., ignoring vertical advection of momentum) and from (b), (d), (f) a vertical integral along a constant angular momentum (m).
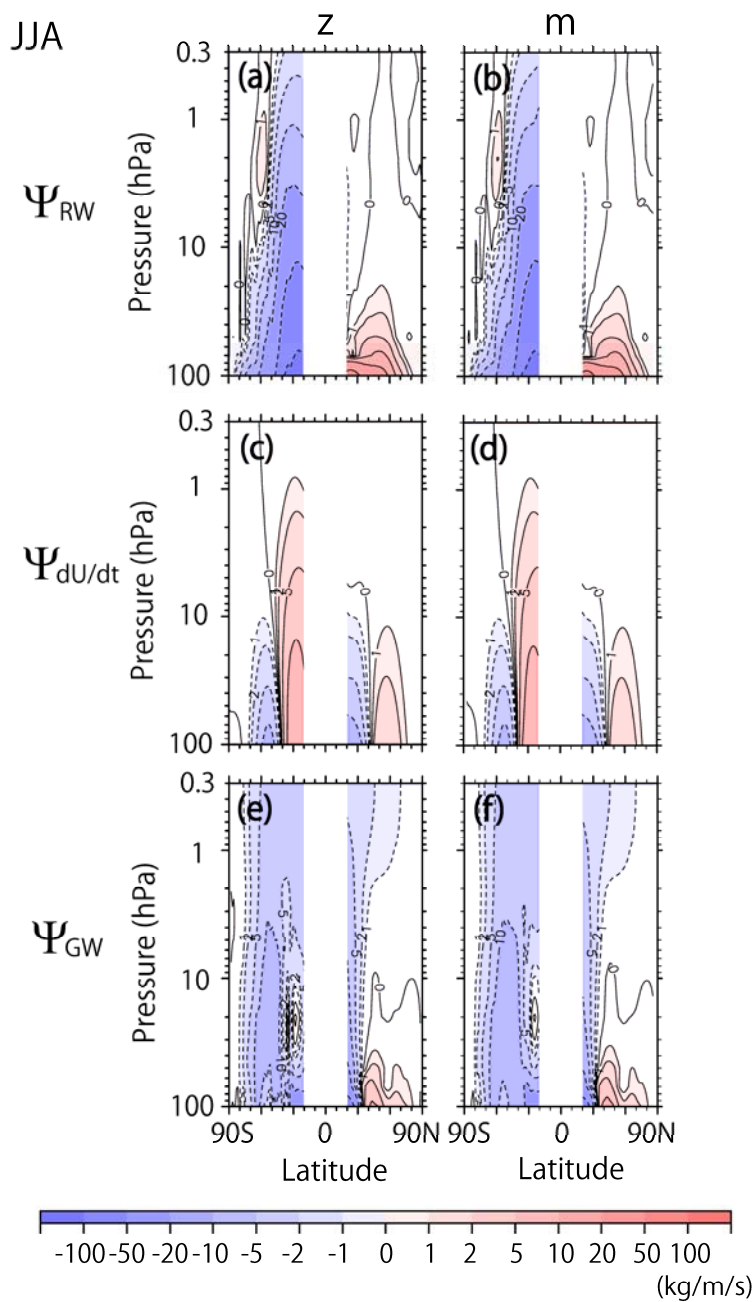
Figure B-2. The same as Figure B-2 but for JJA.